UNIVERSITY OF NAPOLI FEDERICO II

Doctorate School in Molecular Medicine

Doctorate Program in

Genetics and Molecular Medicine

Coordinator: Prof. Lucio Nitsch

XXVI Cycle

"HIGH FAT DIET INDUCES CHROMATIN REMODELLING AND ALTERS THE EXPRESSION OF THE DIABETOGENE *Ped/Pea-15*"

Viviana Vastolo

Napoli 2014

“HIGH FAT DIET INDUCES CHROMATIN REMODELLING AND ALTERS THE EXPRESSION OF THE DIABETOGENE *Ped/Pea-15*”

TABLE OF CONTENT

LIST OF PUBLICATIONS

This dissertation is based upon the following publication:

1. Ungaro P, Mirra P, Oriente F, Nigro C, Ciccarelli M, Vastolo V, Longo M, Perruolo G, Spinelli R, Formisano P, Miele C, Beguinot F. **Peroxisome proliferator-activated receptor-γ activation enhances insulin-stimulated glucose disposal by reducing ped/pea-15 gene expression in skeletal muscle cells: evidence for involvement of activator protein-1.** *J Biol Chem. 2012 Dec 14;287(51):42951-61*

ABSTRACT

Environmental factors interact with the genome to influence gene expression, tissue function and also disease risk. External stimuli may affect the phenotype through epigenetic mechanisms that provide an interface with the genome. Phosphoprotein Enriched in Diabetes/ Phosphoprotein Enriched in Astrocytes (*Ped*/*Pea-15*) is a gene commonly overexpressed in Type 2 Diabetes individuals and in their euglycaemic offspring. Furthermore, its overexpression impairs glucose tolerance and insulin sensitivity in transgenic mouse models. However, whether external cues can affect its expression remains unclear. Therefore, the aim of this study is to evaluate whether the administration of a high fat diet (HFD) in mice could affect *Ped*/*Pea-15* expression and whether chromatin remodelling and epigenetic modifications take part in this regulation. In this work, I demonstrated that high fat diet increases *Ped*/*Pea-15* levels in the skeletal muscle and adipose tissues but not in the liver, accompanied by a chromatin reorganization assessed by Formaldehyde Assisted Isolation of Regulatory Elements (FAIRE) assays. Moreover, chromatin remodelling upon high fat diet does not result in nucleosome depletion but in changes in histone modifications. In particular, increased gene transcription well correlates with increased H4 acetylation and histone H3 dimethylation of lysine 4 on *Ped*/*Pea-15* promoter, two active histone marks. In addition, a specific promoter region acquires typical features of enhancer elements such as monomethylated lysine 4 (H3K4me1) and acetylated lysine 27 (H3K27Ac) on histone H3 in the skeletal muscle tissue of HFD mice compared to STD mice. These two histone marks lack instead in the liver of both HFD and STD mice. These findings provide evidence for environmentally induced changes at *Ped*/*Pea-15* promoter and, for the first time, highlight the presence of a distal, tissue-specific, regulatory element potentially involved in the upregulation of *Ped*/*Pea-15* upon high fat diet administration.

Since direct evidence linking specific environmental cues and metabolic disorders are still limited, addressing this issue will provide new insight into the molecular basis of type 2 diabetes as well as create novel translational perspective.

1. BACKGROUND

1.1 Epigenetics

Genetic information encoded in DNA is largely identical in every cell of an eukaryote. However, cells in different tissues and organs can have widely different gene expression patterns and can exhibit specialized functions. Moreover, specific gene expression patterns need to be appropriately induced and maintained and also need to respond to developmental and environmental changes. Therefore, most of the differences among specialized cells are epigenetic and non genetic.

The word "epigenetics" was termed in the early 1940s to describe the events that could not be wholly explained by traditional genetics. Conrad Waddington defined epigenetics as "*the branch of biology which studies the causal interactions between genes and their products which bring the phenotype into being*" (Choudhuri, 2011). The epigenetic field now actively uncovers the molecular mechanisms underlying these phenomena, and epigenetics has been defined today as "the study of changes in gene function that are mitotically and/or meiotically heritable and that do not entail a change in DNA sequence" (Jaenisch & Bird, 2003). In other words, epigenetics is the study of changes in gene expression or phenotype, caused by mechanisms other than DNA sequences.

1.2 Epigenetic modifications

The first types of epigenetic systems are the chromatin-marking system and the DNA methylation system, referred as "epigenetic *marks*". The most studied epigenetic modifications include DNA methylation, noncoding RNAs and histones modifications.

DNA methylation occurs principally at a cytosine base, mainly in CpG dinucleotides in vertebrates; it is a simple covalent chemical modification, resulting in the attachment of a methyl (CH3) group at the 5' carbon position of the cytosine ring. Generally, DNA methylation is associated with gene repression (de Groote et al, 2012; Maunakea et al, 2010).

Noncoding RNAs (ncRNAs) are another type of epigenetic actors (Morris, 2009). NcRNAs regulate gene expression by *cis*- and *trans*-acting mechanisms (Rassoulzadegan et al, 2006). Some ncRNAs act in concert with components of chromatin and the DNA methylation machinery to establish and/or sustain gene silencing (Zaidi et al, 2011). They can also regulate RNA processing, mRNA stability, translation, and protein stability and secretion. Indeed, they can

contribute to gene splicing, nucleotide modification protein transport and regulation of gene expression. Non coding-RNAs include micro-RNAs (miRNAs) that can regulate gene expression by post-translational silencing of gene expression and long noncoding RNAs (lncRNAs) can act as tethers and guides to bind proteins responsible for modifying chromatin and mediate their deposition at specific genomic locations (Kawaji et al, 2008).

Finally, a large number of different post-translational modifications (PTMs) can occur on histone tails. These modifications affect inter-nucleosomal interactions and thus affect the overall chromatin architecture contributing to the control of gene expression through influencing chromatin compaction or signaling to other protein complexes (Kouzarides, 2007).

1.2.1 Histone modifications

DNA in eukaryotic cells is organized in a DNA-protein complex known as chromatin. Nucleosome is the fundamental unit of chromatin and it is composed of two copies each of the four core histone proteins (H3, H4, H2A, H2B) around which 147 base pairs of DNA are wrapped (Wellen et al, 2009) (Figure 1). The organization into nucleosomal arrays only results in a 5-fold compaction of DNA. The linker histone H1 is associated with the linker DNA as well as with the nucleosome core particle itself, and thus plays an important role in the compaction of DNA beyond the nucleosomal level.

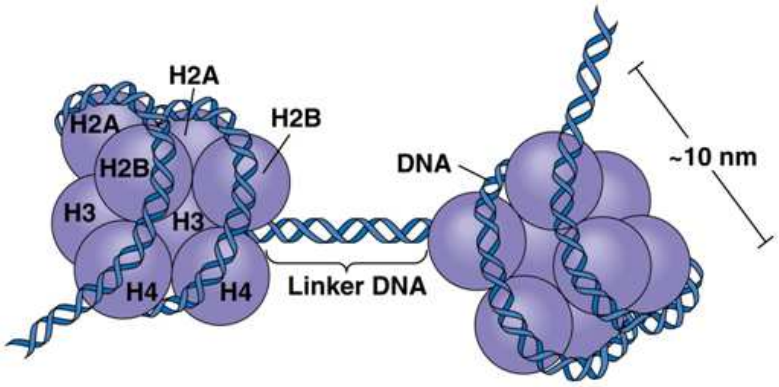

Figure1. Eukaryote genome packaging: A histone octamer is the eight protein complex found at the center of a nucleosome core particle. It consists of two copies of each of the four core histone proteins (H2A, H2B, H3 and H4) surrounded by 147 base pairs of DNA wrapped in a superhelical. The organization into nucleosomal arrays results in a 5-fold compaction of DNA (10-nm fibre). The linker histone H1 is associated with the linker DNA as well as with the nucleosome core particle itself, and thus plays an important role in the higher compaction of DNA (30-nm fiber).

For long time, chromatin was thought to have a primarily structural role, allowing compaction of DNA within the nucleus. It is now clear that chromatin structure is dynamic and that it regulates a number of processes essential for normal cellular functions, including gene transcription, DNA replication, repair, and recombination (Latham & Dent, 2007). Chromatin structure is regulated primarily through dynamic modifications of the histone proteins. Therefore, histone post-translational modifications can control the packaging of DNA and therefore, strongly contribute to the control of gene expression (Greer & Shi, 2012; Kouzarides, 2007).

As mentioned above, DNA is packaged around histone proteins. The core histones are predominantly globular except for their N-terminal *tails* which are unstructured. The histone N-terminal tails protrude from nucleosome cores and thus are subject to numerous modifications by histone modifying enzymes, resulting in acetylation, methylation, phosphorylation, sumoylation, ubiquitylation, ADP ribosylation, deimination and proline isomerization (Kouzarides, 2007) (Figure 2).

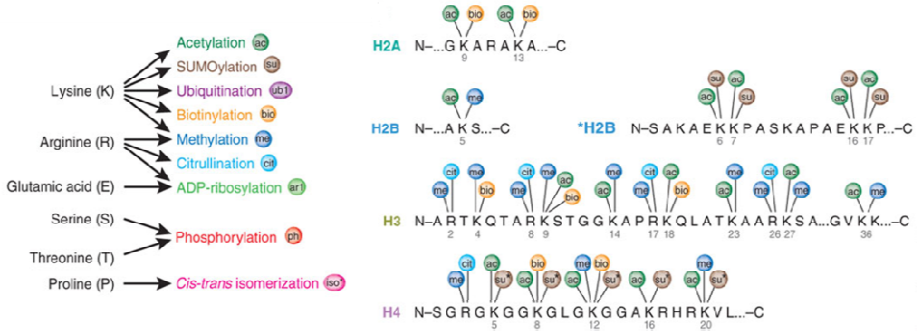

Figure 2. Post-translational modifications of nucleosomal histones. Most of the known histone modifications occur on the N-terminal tails of histones, with some exceptions including ubiquitination of the C-terminal tails of H2A and H2B and acetylation and methylation of the globular domain of H3 at K56 and K79, respectively. Globular domains of each core histone are represented as colored ovals.

Over than 60 different residues have been detected on which histones can be modified (Liu et al, 2005; Pokholok et al, 2005). However, this represents a huge underestimate of the number of modifications that can take place on histones. Thus, depending on the composition of modifications on histones, regulatory protein are encouraged to bind or are occluded from chromatin, thereby influencing gene expression. The most studied histone modifications so far are methylation, acetylation and phosphorylation.

Methylation is the most complicated histone modification. This complexity comes partly from the fact that methylation can occur at lysines, arginines or

histidines residues and it may be one of three different forms: mono-, di-, or trimethyl for lysines, mono- or di- (asymmetric or symmetric) for arginines, and histidines have been reported to be monomethylated (Greer & Shi, 2012). The most extensively studied histone methylations include that on lysine and arginine residues on histones H3 and H4. However, many other basic residues throughout all the histone proteins have also been described (Young et al, 2010). In general, histone methylation is more stable than other PTMs, and it was originally thought to be irreversible. However, the discovery of a demethylase revealed that it is, in fact, reversible (Shi et al, 2004). Both lysine and arginine methylation can be either activating or repressive for gene expression (Bannister & Kouzarides, 2005; Lee et al, 2005). Regarding lysine methylation, three sites are implicated in activation of transcription: H3K4, H3K36 and H3K79. In contrast, H3K9, H3K27 and H4K20 are associated to gene repression. More specifically, lysine 4 can be mono-, di- and tri-methylated. To this regard, a particular insight is the correlation between some chromatin marks and specific regulatory elements. Indeed, promoter regions are marked by trimethylation (H3K4me3) and associated with RNA polymerase II, while distant regulatory regions - like enhancers- are characterized by the monomethylation at the same position (H3K4me1) (Visel et al, 2009). Moreover, many H3K4me1 marked regions can gain the H3K27 acetylation mark, probably recruiting histone acetyltransferases such as p300. This additional mark results in a switch from a "poised" to "active" status of distal regulatory elements (Ostuni et al, 2013).

Regarding histone acetylation, of all the known modifications, has the most potential to unfold chromatin since it neutralizes the basic charge of the lysine. Acetylation occurs at lysine residues on the amino-terminal tails of the histones, thereby neutralizing the positive charge of the histone tails and decreasing their affinity for DNA (Struhl, 1998). As a consequence, histone acetylation alters nucleosomal conformation which can increase the accessibility of transcriptional regulatory proteins to chromatin templates (Kouzarides, 2007). Thus this modification is almost invariably associated with activation of transcription. Moreover, it has been demonstrated that acetylation of H4K16 has a negative effect on the formation of a 30-nanometer fiber and the generation of higher-order chromatin structures (Shogren-Knaak et al, 2006).

Phosphorylation is another modification that may well have important consequences for chromatin compaction via charge changes. Some evidence highlights it in mitosis, apoptosis, and gametogenesis (Rossetto et al, 2012).

This vast array of modifications gives enormous potential for functional responses, but not all these modifications will be on the same histone at the same time (Siebel et al, 2010). The timing of the appearance of a modification will depend on the signaling conditions within the cell. Moreover, these modifications regulate one another, providing regulatory cross-talk (Latham & Dent, 2007). Thus, one modifications can influence the occurrence of one or more subsequent modifications either *in cis*, on the same histone molecule, or *in trans*, between histone molecules or across nucleosomes (Figure 3).

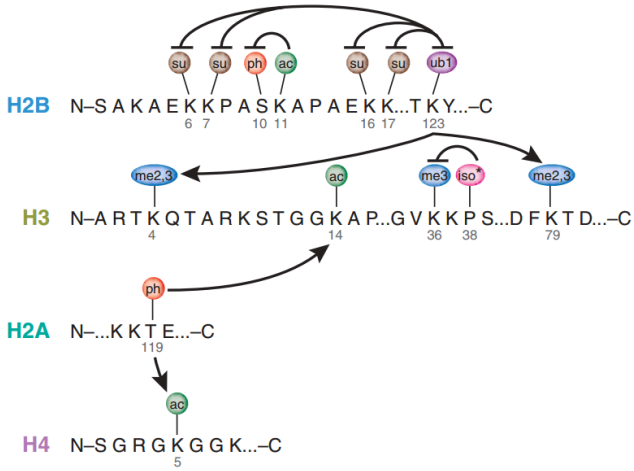

Figure 3 Cross-talk between histone modification *in cis* and *in trans*. Modifications on histone tail makes a cross-talk between different residues. The positive influence over another is shown by an arrow and the negative effect by a dish-line.

The histones-DNA interactions set a critical stage for the regulation of the transcription of genes by influencing the DNA accessibility to the cell transcriptional machinery elements. In this scenario, all the post-translational modifications of histone proteins, also known as *histone code*, provide a platform to accommodate the binding of factors regulating the chromatin function. Therefore, alterations in these epigenetic modifications could lead to the deregulation of gene transcription.

1.3 Epigenetics as a link between metabolism and transcription

Metabolic homeostasis is maintained by tightly controlled transcriptional mechanisms. In turn, transcriptional control is achieved through complex molecular events in which take part transcription factors, the basal transcriptional machinery and co-regulatory proteins (Feige & Auwerx, 2007). These co-regulators are proposed to act as *metabolic sensors*, able to translate

change in metabolism into change in gene expression by affecting the activity of transcription factors, as well as changing the structure of the epigenome (Haberland et al, 2009). In particular, nutritional information may influence the epigenome by directly affecting the activities of epigenetic modifiers (Teperino et al, 2010). For example, the loss of function of the histone demethylase, *Jhdm2a*, associated with obesity, decreased the expression of metabolically active genes in the skeletal muscle tissue, and impaired cold-induced *uncopling protein 1* expression in brown adipose tissue in rodents (Tateishi et al, 2009). Moreover, the nicotinamide adenine dinucleotide (NAD+)-dependent *sirtuins* are involved in epigenetic controls of metabolism (Schwer & Verdin, 2008). Indeed, energy-rich substrates (e.g. carbohydrates, fat) are converted into ATP increasing the levels of some metabolites, such as acetyl-CoA, nicotinamide adenine dinucleotide (NAD+), S-Adenosyl-methionine (SAM), alpha-ketoglutaric acid and flavin adenosine dinucleotide.

These metabolities are used as coenzymes by chromatin-modifying enzymes. For example, all the three classes of histone methyltransferases use S-Adenosyl-methionine to transfer methyl groups (Smith & Denu, 2009). Indeed, also demethylases use metabolites as cofactors; lysine-specific demethylase 1 (*LSD-1*) is FAD-dependent, whereas *JmjC* enzymes feature α-ketoglutarate-dependent activity (Shi et al, 2004; Tsukada et al, 2006). Moreover, it has recently been suggested that glucose availability can affect histone acetylation in an ATP-citrate lyase-dependent manner, further linking metabolic homeostasis to epigenetic regulation (Wellen et al, 2009).

Thus, metabolic deregulation alters coenzymes biosynthesis that, in turn, affects the activity of chromatin modification enzymes leading to an alteration in gene expression.

Therefore, epigenetics may play a key role in the causation and in the progression of many common multifactorial diseases, such as diabetes and obesity, both associated with an aberration of cellular energy metabolism.

1.4 Type 2 Diabetes

Type 2 diabetes (T2D) is a disease of impaired glucose homeostasis and insulin action with an etiology that encompasses genetic, cellular and environmental factors. It results from the imbalance between glucose production and glucose utilization reflecting the imbalance between insulin resistance of muscle, adipose tissue, and liver and the secretion of insulin by the β-cells mass (Lin & Accili, 2011; Taylor, 2008; Weyer et al, 1999) (Figure 4).

T2D is the most common type of diabetes, accounting for 90% of all forms of the disease. It is typical of the adult age, but it is now also increasing among young adults. Rarely, T2D is an isolated condition; it is most often one of set of features called metabolic syndrome, including obesity, hypertension, dyslipidemia.

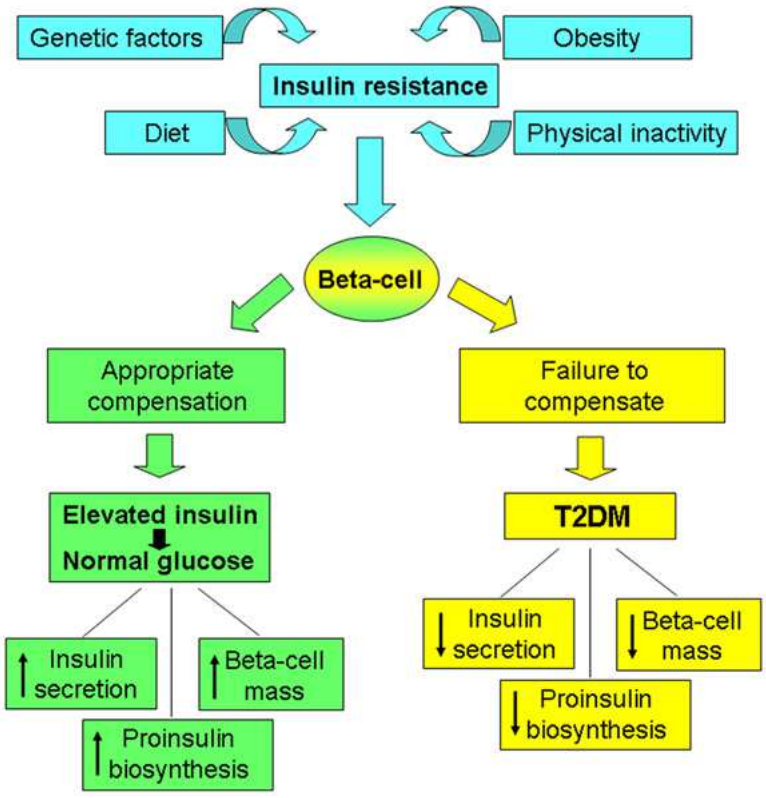

Figure 4 Factors involved in pathophysiology of type 2 diabetes Both genetic and environmental factors cooperate in the development of insulin resistance. At the onset of the disease, β-cells increase insulin release to overcome the reduced efficiency of insulin action, thereby maintaining normal blood glucose level. By contrast, when β-cells fail to compensate, impaired glucose tolerance and, finally, type 2 diabetes occur.

As mentioned above, type 2 diabetes is a complex trait influenced by genetic and environmental factors. The identification of the genes involved in T2D has been an arduous task for geneticists, devoting a large amount of effort to this goal. Thus, several candidate-gene studies have been performed that were successful in identifying some monogenic familial forms of T2D such as maturity onset diabetes of the young (MODY), mitochondrial diabetes and neonatal diabetes (Barroso, 2005). Unfortunately, these monogenic forms of diabetes represent only a small fraction of the disease. However, linkage and associations studies on common form of T2D provided inconsistent results.

Only *PPARg*, *KCKJ11* and *TCF7L2* were identified as established genes associated with the frequent forms of the disease (Zeggini, 2007).

Thereafter, genome-wide association studies (GWASs) were supposed to provide a novel understanding of T2D causation. Multiple loci markers have been found through these studies that heightens risk for T2D when present (Sanghera & Blackett, 2012). While GWAS has enabled the generation of new hypotheses regarding the relation of genetics to T2D, the genetic markers found have poor penetrance. Further, these genetic markers do not explain a significant portion of T2D in context of other factors. Perhaps the lack of impact of GWAS comes from not comprehensively considering environmental factors in the disease. Indeed, while genetics play a large role, specific environmental factors are also emerging as risk factors for the disease.

Environment is even more complex than genetics, since it is made of a continuous flow of space-time exposures from the time of one-cell zygote to the time of disease onset. A first environmental-wide association study (EWAS) was performed in a T2D cohort and identified potential environmental factors with effect sizes comparable to loci found by GWAS (Patel et al, 2010). Environmental contributions to the development of type 2 diabetes potentially include exposures such as a suboptimal *in utero* environment, low birth weight, obesity, nutrients, inactivity, advancing age. These environmental perturbations can lead to a disease phenotype by affecting gene expression through epigenetic modifications.

Moreover, the incidence of type 2 diabetes has rapidly increased over the past several decades and is now reaching epidemic proportions across the globe. The World Health Organization (WHO) has declared that a diabetes epidemic is underway. In 1985, an estimated 30 million people worldwide had diabetes. By 1995, this number had shot up to 135 million, and by 2005 reached an estimated 217 million. Alarmingly, the WHO predicts that this will increase to at least 366 million by 2030 (Smyth & Heron, 2006).

The threatened epidemic of T2D is largely driven by the increase in obesity. Both, obesity and type 2 diabetes are becoming the *normal* metabolic fate of a large fraction of human populations. This escalation in frequency certainly has a widespread genetic background, but several evidence suggest its main sources in environmental changes. In addition, genetic models to explain the epidemic obesity are inadequate because the emergence over the past 30 years has been too rapid to allow for the appearance of new mutant genes. Accordingly, epigenetic modifications of gene structure through nutritional and physiological stress provide mechanisms for inducing obesity and type 2 diabetes that are independent of new mutations to the genome. For these

reasons, epigenetics has become a leading causative candidate for the causation, and possibly inheritance, of obesity and type 2 diabetes. However, the knowledge about epigenetic mechanisms associated to type 2 diabetes still remains limited. Therefore, it will be a great challenge addressing this issue, making possible to test epigenetic drugs as a putative novel treatment of diabetes as well as its complications.

1.4.1 *Ped/Pea-15* gene

Posphoprotein Enriched in Diabetes/Phosphoprotein Enriched in Astrocytes (*Ped/Pea-15*) gene maps on human chromosome 1q21-22, is highly conserved among mammals, and is ubiquitously expressed in human tissues (Danziger et al, 1995). It encodes for a 15-kDa cytosolic multifunctional protein. Indeed, PED/PEA-15 protein has initially been identified in [32P]phosphate-labeled astrocytes and for this reason it was named Phosphoprotein Enriched in Astrocytes (Araujo et al, 1993). Using a differential cloning strategy, PED/PEA-15 was later found to be overexpressed in skeletal muscle and fat tissues as well as in cultured skin fibroblasts of type 2 diabetic subjects, but not in type 1 diabetic patients (Condorelli et al, 1998). Therefore, it has been renamed Phosphoprotein Enriched in Diabetes.

PED/PEA-15 is a scaffold protein regulating the function of a number of signaling proteins and effectors. It is highly regulated and it can be phosphorylated at Ser_{104} by protein kinase C and at Ser_{116} by calcium-calmodulin kinase II (CaMKII) and by Akt/PKB. Thus, PED/PEA-15 exists in three differentially phosphorylated forms: unphosphorylated, mono-phosphorylated and bi-phosphorylated. It exerts a broad anti-apoptotic function by interfering with both intrinsic and extrinsic pathways (Condorelli et al, 2002; Condorelli et al, 1999; Peacock et al, 2009; Trencia et al, 2004). In addition, PED/PEA-15 is involved, at least in part, in the regulation of cellular proliferation by controlling the extracellular signal-regulated kinase (ERK) pathway (Callaway et al, 2007; Formstecher et al, 2001). There are also evidence in literature regarding the role of PED/PEA-15 in neoplastic transformation. Indeed, in tumors driven by oncogenic *Ras*, PED/PEA-15 acts as an ERK1/2 nuclear export factor and exerts tumor suppressor activity (Gaumont-Leclerc et al, 2004). On the other hand, it has been demonstrated that high levels of PED/PEA-15 expression associate with development of malignancy: *Ped/Pea-15* gene is overexpressed in human gliomas and in mammary carcinomas (Hao et al, 2001; Hwang et al, 1997; Stassi et al, 2005; Xiao et al, 2002). It is possible that the differences in the effects mediated by PED/PEA15 could depend on its phosphorylation state and on the cellular

context. Finally, *Ped/Pea-15* emerged as a key regulator of glucose metabolism.

1.4.2 PED/PEA-15 and glucose metabolism

Earlier findings in humans evidenced that *Ped/Pea-15* gene is overexpressed in skeletal muscle and fat tissues as well as in cultured skin fibroblasts from individuals with type 2 diabetes (Condorelli et al, 1998). Indeed, *Ped/Pea-15* overexpression represents a common trait among type 2 diabetics, because approximately one-third of the individuals diagnosed with the disorder exhibit *Ped/Pea-15* expression levels higher than 2 SD above the mean in the control subjects (Condorelli et al, 1998).

Further functional analysis in cultured skeletal muscle and adipose cells demonstrated that increased expression of PED/PEA-15 causes resistance to insulin action in glucose uptake. In particular, PED/PEA-15 binds phospholipase D1 (PLD1) and enhances its stability and activity thus increasing diacylglycerol (DAG) levels, thereby activating the dyacylglycerol-sensitive protein kinase C α (PKCα). This effect, in turn, prevents the activation of the PKCζ isoform, a major activator of glucose transporter 4 (GLUT4) vescicle translocation toward the plasma membrane (Condorelli et al, 2001; Zhang et al, 2000) (Figure 5).

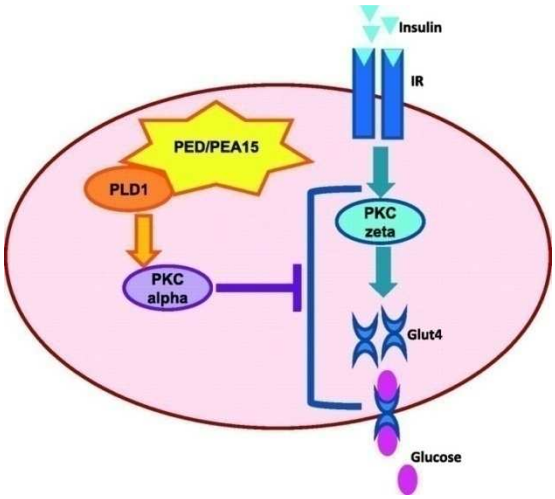

Figure 5 Role of PED/PEA-15 in glucose metabolism. Overexpression of PED/PEA-15 binds phospholipase D, thereby increasing its stability and diacylglycerol levels. The consequent increase of PKCα activation leads in turn to the inhibition of PKCζ responsible for the glucose transporter 4 (GLUT4) translocation, impairing insulin-induced glucose uptake.

To better address the effects of PED/PEA-15 over-expression on glucose tolerance a transgenic mouse has been generated, ubiquitously over-expressing *Ped/Pea-15* gene. This mouse model exhibits mildly elevated random-fed blood glucose levels and becomes hyperglycemic after glucose loading, indicating that increased expression of this gene is sufficient to impair glucose tolerance (Vigliotta et al, 2004). Indeed, *Ped/Pea-15* transgenic mice are much more insulin resistant than their nontransgenic littermates. The transgenic mice were consistently markedly hyperinsulinemic in the basal state and exhibited increased free fatty acid levels in blood. The transgenic mice also show reduced insulin response to a glucose challenge, indicating that the overexpression of *Ped/Pea-15* impairs insulin secretion in addition to insulin action (Vigliotta et al, 2004).

Moreover, to clarify the role of PED/PEA-15 in the glucose-regulated insulin secretion, it has been generated the transgenic mice over-expressing *Ped/Pea-15* selectively in β-cells. This animal model shows impaired glucose tolerance and reduced insulin secretion in response to hyperglycemia. This latter defect is comparable with that occurring in mice with ubiquitous overexpression, suggesting that β-cell overexpression of *Ped/Pea-15* is sufficient to impair glucose tolerance in mice (Miele et al, 2007). Additional studies in *Ped/Pea-15* null mice revealed that the ablation of even a single copy of the gene is able to increase the insulin sensitivity (*unpublished data*).

All these findings suggest that PED/PEA-15 has an important role in the control of insulin sensitivity and therefore its abnormalities provide a strong contribution to insulin resistance.

Interestingly, it has been demonstrated that increased levels of PED/PEA-15 also occur in euglycaemic subjects with diabetic first-degree relatives (FDR) respect to euglycaemic subjects with no family history of diabetes (Valentino et al, 2006). In addition, in nondiabetic offspring of type 2 diabetics from the European Network on Functional Genomics of Type 2 Diabetes (EUGENE2) cohort, PED/PEA-15 expression levels strongly correlate with insulin resistance (Valentino et al, 2006).

As outlined above, *in vitro* and *in vivo* studies have clearly demonstrated the close relationship between *Ped/Pea-15* over-expression and the impaired insulin action and secretion. However, the mechanisms through which this alteration in gene expression occurs are not fully elucidated.

1.4.3 Ped/Pea-15 transcriptional regulation

First evidence suggested that overexpression of *Ped/Pea-15* in the diabetics may be caused by transcriptional abnormalities since no mutations were

detected by denaturing gradient gel electrophoresis (DGGE) in the coding region of the gene in 23 type 2 diabetic individuals analyzed (Condorelli et al, 1998).

To get further insight in *Ped/Pea-15* transcriptional regulation, its promoter has been characterized, obtaining evidence that the balance between *Chicken Ovalbumin Upstream Promoter Transcription Factor II* (COUP-TFII) and *Hepatocyte Nuclear Factor 4α* (HNF-4α) could regulate, at least in part, its transcription acting as positive and negative regulators, respectively (Ungaro et al, 2008). In addition, both these factors are involved in the control of glucose homeostasis (Hayhurst et al, 2001; Pereira et al, 2000; Xanthopoulos et al, 1991). Thus, abnormalities in their balance might have important consequences on glucose tolerance. Nevertheless, polymorphisms in their consensus binding sequence may affect *Ped/Pea-15* expression, thereby increasing the susceptibility to type 2 diabetes. Further studies revealed that HNF-4α represses *Ped/Pea-15* expression by triggering *Silencing Mediator of Retinoic acid and Thyroid hormone receptor* (SMRT) recruitment to the gene promoter and thereby, leading to histone deacetylation-associated remodelling of chromatin (Ungaro et al, 2010).

More recently, it has been demonstrated that *Peroxisome Proliferator-Activated Receptor-γ* (PPARγ) represses transcription of the *Ped/Pea-15* gene, identifying it as a novel downstream target of a major PPARγ-regulated inflammatory network (Ungaro et al, 2012). In this context, it is well known that thiazolidinediones markedly improves insulin sensitivity in type 2 diabetic patients acting through peroxisome proliferator-activated receptor-γ (PPARγ) mediated mechanisms. Therefore, *Ped/Pea-15* repression may contribute to thiazolidinediones action on glucose disposal. In addition, further results indicate that PPARγ regulates *Ped/Pea-15* transcription by inhibiting c-JUN binding at its promoter (Ungaro et al, 2012). Accordingly, JNK/AP1 network together with NF-κB pathway are activated in classical insulin target tissues as a consequence of the chronic low grade inflammation, typical of both obesity and type 2 diabetes. (Bandyopadhyay et al, 2005; Itani et al, 2002; Osborn & Olefsky, 2012).

However, whether the overexpression occurring in type 2 diabetic individuals is determined exclusively by genetic mechanisms and/or whether non genetic mechanisms may also contribute are issues that still remain to be established.

Elucidating how the *Ped/Pea-15* gene is regulated could generate further insight into the molecular bases of diabetes as well as novel translational perspectives.

2. AIMS OF THE STUDY

Type 2 diabetes (T2D) is a metabolic disorder resulting from the complex interaction between genetic and environmental factors. It is a growing health problem worldwide and genetic models to explain its epidemic are inadequate because its increase has been too rapid to allow for the appearance of new mutant genes. In addition, increasing evidence show that environmental cues, such as fat-enriched diet, strongly contribute to development and progression of multifactorial disease, by altering gene expression through epigenetic modifications.

Ped/Pea-15 gene is widely expressed in different tissues and highly conserved among mammals. It has emerged as an important regulator of insulin sensitivity. Indeed, *Ped/Pea-15* is overexpressed in skeletal muscle and adipose tissues of type 2 diabetic individuals, as well as in white blood cells from non diabetic individuals with a strong family history of type 2 diabetes.

However, whether the overexpression of *Ped/Pea-15* gene is determined exclusively by genetic mechanisms and/or whether non genetic mechanisms may also contribute are issues that still remain to be established.

Based on this knowledge, the aim of this work is to clarify whether and how external stimuli, such as the administration of a high fat diet, could impact on *Ped/Pea-15* expression in insulin target tissues and whether chromatin remodelling and epigenetic modifications can play a role in the regulation of this candidate gene.

The knowledge about the molecular mechanisms linking environmental factors and type 2 diabetes are still limited, so far. Therefore addressing this issue will provide some insights into epigenetic mechanisms associated with type 2 diabetes.

3. MATERIALS AND METHODS

3.1 Animal study

Male C57Bl6/J mice were hosted at the common facility of the University of Naples Medical School. They were housed 5 per cage under the conditions of constant temperature (22°C), a light/dark cycle of 12 h with free access to food and water. Diet protocol started when mice where 7-week-old. For high fat diet (HFD) treatment, mice were fed a high fat diet with ~ 60 cal % fat or a standard diet with ~ 10 cal % fat (Research Diets, New Brunswick, NJ) for 22 weeks.

All the experiments performed on mice were conducted in accordance with the Principles of Laboratory Care.

3.2 Glucose Tolerance Test (GTT)

The test was performed at the beginning and at the end of the diet protocol. Mice were fasted overnight and then injected with 2g/kg body weight of glucose. Blood samples were taken from mice tail and glycaemia was analyzed by using a glucose analyzer (LifeScan). Glucose levels were determined at the following time points: 0, 15, 30, 45, 60, 90, 120 min after glucose injection.

3.3 Insulin Tolerance Test (ITT)

The test was performed at the beginning and at the end of the diet protocol. Insulin sensitivity was assessed on 5 hr starved mice and then injected with 0,75 U/kg body weight of insulin. Blood samples were taken from mice tail and glycaemia was analyzed by using a glucose analyzer (LifeScan). Glucose levels were determined at the following time points: 0, 15, 30, 45, 60, 90, 120 min after insulin injection.

3.4 Glucose-Stimulated Insulin Secretion (GSIS)

The test was performed upon 22 weeks of diet protocol on overnight fasted mice. Animals were intraperitoneally injected with 3g/kg body weight of glucose. In parallel, blood samples were taken from mice tail, to assess glycaemia, and from orbital sinus in order to collect large volumes of blood to further measure serum insulin. Animals received topical anesthetic during this procedure (tetracaine ophthalmic drops). Blood samples were collected at 0, 3 30 min after glucose injection. Blood samples were centrifuged at 1500 *rpm* for 20 min at room temperature and serum collected. Insulin levels were measured

with radioimmunoassay (RIA) kit (#RI-13K, Millipore), according to the manufacturer's protocol.

3.5 Biochemical parameters

In overnight fasted mice, analyses of serum triglycerides, total cholesterol, HDL, LDL, were done by using Horiba ABX Pentra400 Chemistry Analyzer (HORIBA ABX, Montpellier, France).

3.6 Western Blot Analysis

Tissues were weighed and total proteins were extracted in JS buffer (Hepes 1 M pH 7.5, NaCl 5 M, glycerol 100%, Triton x-100 1%, $MgCl_2$ 1 M, EGTA 0,1M), supplemented with the Complete Protease Inhibitor Mixture Tablets (Roche Applied Science). After lysates clarification, protein concentration was determined using Bradford assay (Bio-Rad). Protein extracts (200 μg skeletal muscle- 50 μg liver- 100 μg adipose tissue) were resolved by SDS-PAGE and blotted on nitrocellulose membranes (Millipore, Billerica, MA). Nonspecific binding was blocked with 5% nonfat milk for 1 h at the room temperature. Bands were visualized by reacting with specific antibodies which were revealed by chemio-luminescence (Amersham, Biosciences). The following antibodies were used: rabbit anti-PEA-15 (#2780 Cell Signaling) and mouse anti-α-tubulin (T5168 Sigma), as loading control.

3.7 Real time PCR

70mg of tissue were weighed and total RNA was isolated using Trizol reagent (Aurogene), according to the manufacturer's protocol. The cDNA synthesis was generated from 1 μg of total RNA by using Superscript II (Invitrogen, Life Technologies) in a 20 μl reaction volume. After cDNA synthesis, Real time PCR was performed on CFX96 (Biorad) in a final volume of 10 μl containing 20 ng of cDNA, 5 μl of iTaq Universal SYBR Green Supermix (Biorad) and specific forward and reverse primers (Sigma). The sequences of the primers used are listed in Table 1. The *Gapdh* gene was used as internal control and the results of Real time analysis are expressed as the ratio between the copy number variation (CNV) of *Ped/Pea-15* and that of the reference gene.

Table 1 primers sequences used for Real time PCR

GENE NAME	PRIMER SEQUENCES (5'-3')
PED/PEA-15	Forw: ggcagtgcctggtttagcttc Rev: tcagagggctgccggataatg
GAPDH	Forw: aaggcgggggcccacttgaa Rev: tgggtggcagtgatggcatgg

For the analysis of Ped/Pea-15 mRNA levels, target gene expression was measured using the absolute standard curve method for Real time PCR. GAPDH, was used as internal control. Forw: forward primer, Rev: reverse primer

3.7.1 Cloning of the real-time PCR amplification products of *Ped/Pea-15* and *Gapdh* for copy number analysis

For copy number analysis, the real time PCR amplification products for *Ped/Pea-15* and *Gapdh* were cloned into the pGEM-T easy vector (Promega, Madison, WI), according to the manufacturer's protocol. Calibration curves were made from serial 10-fold dilutions of plasmid DNAs, from 1.0 ng/μl to 1.0×10^{-8} ng/μl. The reproducibility of the calibration curves was tested according to the slopes and the correlation coefficients. The mean slopes of the calibration curves for the two genes were similar, -3,3 for *Ped/Pea-15* and -3,1 for *Gapdh*, where a slope of -3,3 ± 10% reflects an efficiency of 100% of the PCR, and the mean correlation coefficient for both curves was 0,99. The copy number of the genes was calculated using the Ct values of the vector and calculating the vector copy number according to the formula (Dhanasekaran et al, 2010; Yuan et al, 2006):

$$Number\ of\ copies = (amount\ (ng) * 6.022 \times 10^{23}) / (length\ (bp) * 1.0 \times 10^{9} * 650)$$

This formula takes into account 6.022×10^{23} (molecules/mole) that is the Avogadro's number and 660 Da that is the average weight of a single base pair (http://cels.uri.edu/gsc/cndna.html).

3.8 Formaldehyde-Assisted Isolation of Regulatory Elements (FAIRE)

Frozen tissues were pulverized into a coarse powder in liquid nitrogen, cross-linked in formaldehyde 1% for 10 min and then quenched with the addition of glycine 125 mM. Following PBS washing, tissues were lysed in ice-cold FAIRE lysis buffer (10 mM Tris-HCl pH 8.0, 2% vol/vol Triton X-100, 1% SDS, 100 mM NaCl, 1 mM EDTA) by using metal beads. The cross-linked chromatin was sheared by sonication (six 30-s cycles with 1-s bursts followed by 0.5 s of rest at 30% amplitude) in order to achieve a range of about 150–750 bp with an average fragment length around 300–400 bp. Lysates were clarified by centrifugation and a 100-μl aliquot was removed to check efficiency of

sonication and to prepare INPUT DNA, used as loading control. The remaining lysate was used to obtain FAIRE DNA. To get INPUT DNA, lysates were treated with DNase-free RNaseA and proteinase K, before phenol/chloroform extraction. Efficiency of sonication was evaluated by running 500 ng INPUT DNA on a 1% (wt/vol) agarose gel and stained with ethidium bromide. FAIRE DNA was prepared, instead, by direct phenol/chloroform extraction and then proteinase K was added to reverse any DNA-DNA cross-links. Both, INPUT and FAIRE DNA were analyzed by semiquantitative PCR, resolved by 2% agarose gel electrophoresis and analyzed by densitometry using the ImageJ software (National Institutes of Health). The sequences of the primers used are listed in Table 2. FAIRE DNA was normalized to INPUT DNA.

Table 2 Primers sequences used to analyze Ped/Pea-15 promoter

Ped/Pea-15 PROMOTER REGION	PRIMER SEQUENCES (5'-3')
mPED_A	Forw: ggaggggtcatgtaaaagca Rev: ggcaggattattcccatcttc
mPED_B	Forw: ggctcaggtgggagtaaaca Rev: ttctgtcgctttccctaagaa
mPED_C	Forw: tccacagtcaaatccaggaag Rev: tgaggcagagcaaaacacag
mPED_D	Forw: ctgtgttttgctctgcctca Rev: cctgagaacggcttcaatgt
mPED_E	Forw: acattgaagccgttctcagg Rev: cacacccccacacactatga
mPED_F	Forw: tcatagtgtgtgggggtgtg Rev: ggaaggcagatcaatttgga
mPED_G	Forw: tccaaattgatctgccttcc Rev: gttcctaagcagcgtctg

PCR primers were designed to produce a series of adjacent partially overlapping PCR products spanning nucleotides -2000 to +165 (distance are relative to transcription start site) of Ped/Pea-15 promoter. A: from -2000 to -1650; B: from -1771 to -1475; C: from -1499 to -1150; D: from -1181 to -803; E: from -823 to -514; F: from -534 to -226; G: from –245 to +162; Forw, forward primer; Rev, reverse primer.

3.9 Micrococcal Nuclease assay (MNase)

Frozen tissues were minced, washed with ice-cold PBS and lysed in ice-cold lysis buffer (10mM Tris pH 7.5, 10mM NaCl, 3mM $MgCl_2$, 0.5% NP-40, 0.15mM spermine, 0.5mM spermidine) by using metal beads. Nuclei were centrifuged at 2000 *rpm* for 5 min at 4°C and resuspended in the MNase digestion buffer (10mM Tris-HCl pH 7.4, 15mM NaCl, 60mM KCl, 0.15mM spermine, 0.5mM spermidine) and the final Ca^{2+} concentration adjusted to 1mM with $CaCl_2$. 0,1 U MNase was added and the reaction mixture was incubated at 37°C for 5 min. An aliquot was removed, as undigested DNA

control. Thus, the reaction was stopped by adding MNase Stop Buffer (20mM EDTA, 20mM EGTA, 0.4% SDS, 0.5mg/mL Proteinase K) and the mixture incubated at 65°C overnight. Both digested and undigested DNA were obtained by direct phenol/chloroform extraction and analyzed by semiquantitative PCR, resolved by 2% agarose gel electrophoresis and analyzed by densitometry using the ImageJ software (National Institutes of Health). MNase digested DNA was normalized to undigested DNA.

3.10 Chromatin Immunoprecipitation assay (ChIP)

Tissues were minced and protein-DNA cross-linked in presence of 1% formaldehyde for 15 min. The cross-linking reaction was stopped by the addition of glycine 125mM. Tissues were lysed and sonicated to achieve chromatin fragments ranging between 500 and 1000 bp in size. The lysates were incubated at 4°C overnight with appropriated antibodies: anti.acetyl-Histone H4 (#06-866, Millipore), anti-dimethyl-Histone H3 (Lys9) (#17-648, Millipore), anti-dimethyl-Histone H3 (Lys4) (#07-030, Millipore), anti histone H3 (#2650, Cell Signaling), anti Histone H3K4me3 (#39915, Active Motif), anti Histone H3K4me1 (#39635, Active Motif), anti-Histone H3K27ac (#39685, Active Motif), anti RNA Pol II (MMS-134R, Covance), anti p300 (#N-15, S. Cruz Biotechnology), anti SET7/9 (#5131-1, Epitomics); normal rabbit serum was used as negative control (#17-684 Millipore). Thus, chromatin-antibody complexes were isolated using protein G/salmon sperm DNA (Millipore, Billerica, MA). Immunoprecipitates and INPUT controls (aliquot separated before immunoprecipitation) were washed and then eluted by freshly prepared 1% SDS, 0.1M $NaHCO_3$ buffer. After reversion cross-linking, DNA was purified by the QIAquick PCR purification kit (Qiagen, Hilden, Germany) followed by PCR amplification. PCR products were resolved by 2% agarose gel electrophoresis, revealed by ethidium bromide staining. Bands were analyzed by densitometry using the ImageJ software (National Institutes of Health); immunoprecipitated DNA signals were normalized to relative input samples and corrected to negative control.

3.11 Statistical analysis

Data are expressed as mean ± SEM. Statistical significance of the differences between groups was determined by two-tailed unpaired Student's t test with the GraphPad prism software (*$p < 0.05$, **$p < 0.01$, ***$p < 0.001$).

4. RESULTS AND DISCUSSION

4.1 Animal study design

It has been well established that the link between obesity and type 2 diabetes is not restricted to humans. When provided to various animal species, high fat diet leads to obesity and induces disease signs that model human type 2 diabetes. Moreover, diet-induced obesity (DIO) in the mouse, in the absence of mutation of selected genes, provide a powerful tool for identifying epigenetic and environmental mechanisms potentially involved.

C57Bl6/J is a well established models for diet-induced obesity; this strain develops severe obesity, hyperglycemia and insulin resistance if weaned onto high fat diet, and therefore it was used for this study.

Animals were acclimated for 3-weeks before experiments and diet protocol started when mice were 7 week-old. Briefly, male mice were used to avoid sex hormones influences and were divided into two groups: 8 mice were fed with a standard diet (10% animal fat) and 8 mice were put on diet-induced obesity regimen (60% animal fat). After 22 weeks of diet protocol, mice were sacrificed and tissues collected (Figure 6).

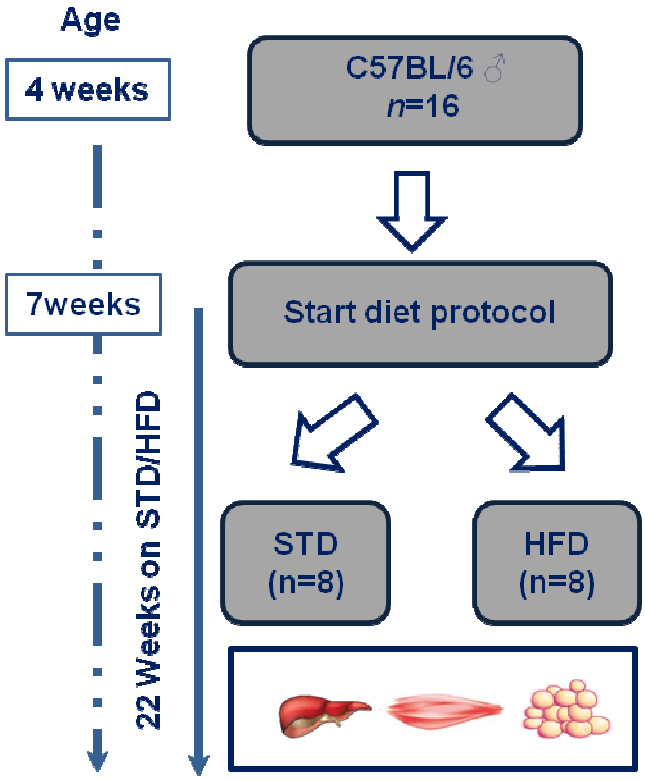

Figure 6 Animal study design for diet-induced obesity. C57Bl6/J male mice were used for diet-induced obesity protocol. Mice were divided into two groups:8 animals were fed a standad diet (STD); 8 animals were fed a high fat diet (HFD). After 22 weeks of diet protocol, mice were sacrificed and tissues collected.

4.2 Metabolic characteristics of standard and high fat mice

Body weight and food intake were weekly evaluated during diet protocol duration. The body weight started to differ between standard mice (STD) and high fat diet mice (HFD) already after two weeks of feeding (25,5 ± 0,4 g STD *vs* 28 ± 0,3 g HFD p-value=$2x10^{-5}$). Figure 7a shows the difference in body weight of STD and HFD mice at the beginning and at the end of diet protocol. HFD mice significantly increased their body weight after 22 weeks of feeding (T_0 24,2 ± 0,4 g *vs* T_{22} 40,9 ± 1,0 g; p-value < 0.001). At variance, STD mice displayed only a mild body weight increase (T_0 24,5 ± 0,4 g *vs* T_{22} 29,5 ± 0,9 g; p-value < 0.05). Concomitantly, food intake was evaluated; food intake was not affected between the two experimental groups (STD 21,2 ± 0,1 g/mouse/day *vs* HFD 20,3 ± 0,3 g/mouse/week) (data not shown). However, the calorie intakes were affected by type of diet (STD 97 ± 7,2 kCal/mouse/week *vs* HFD 189 ± 15,4 kCal/mouse/week; p-value < 0.01).

Thus, I characterized the glucose homeostasis of this mouse model, analyzing the blood glucose levels and the glucose tolerance. Fasting blood glucose was markedly increased in HFD group but not in STD mice (Figure 7b). In addition, during a glucose tolerance test (GTT), glucose loading (2g/kg) rendered HFD mice significantly more hyperglycemic during the following 120 min compared to the STD mice, revealing a strong impairment of glucose tolerance after 22 weeks of feeding (Figure 7c).

Later, I also performed an insulin tolerance test (ITT); after intraperitoneal insulin injection (0.75mU/g) HFD mice displayed reduced insulin sensitivity compared to the control mice (Figure 7d). Therefore, upon 22 weeks of high fat diet administration mice become both glucose intolerant and insulin resistant. Moreover, I performed a glucose-stimulated insulin secretion (GSIS) test to evaluate the appropriate secretion of insulin from pancreatic β-cells (Figure 7e). It is well known that glucose induces insulin secretion in a biphasic pattern: the first phase, which culminates after 5-6 minutes after stimulation, and the second phase, characterized by a gradual increase over 60 min (Seino et al, 2011). Loss of first-phase secretion and reduced second-phase secretion are characteristic features of type 2 diabetes mellitus (T2DM). Thus, the analysis of GSIS revealed that HFD mice are hyperinsulinemic in the basal state compared to control mice; indeed, both the first and the second fases are absent upon glucose stimulation.

Furthermore, as shown in Table 3, over 22 weeks of feeding HFD mice have significantly elevated total cholesterol, LDL and HDL; the increase of this last parameter is probably due to a compensatory effect. At variance, triglycerides levels did not differ between STD and HFD mice. The unchanged triglycerides levels are in accordance with data already published in literature. Indeed, hypertriglyceridemia, even though is closely associated with insulin resistance, is not induced in mice upon HFD administration (Buhman et al, 2000; Kirk et al, 1995).

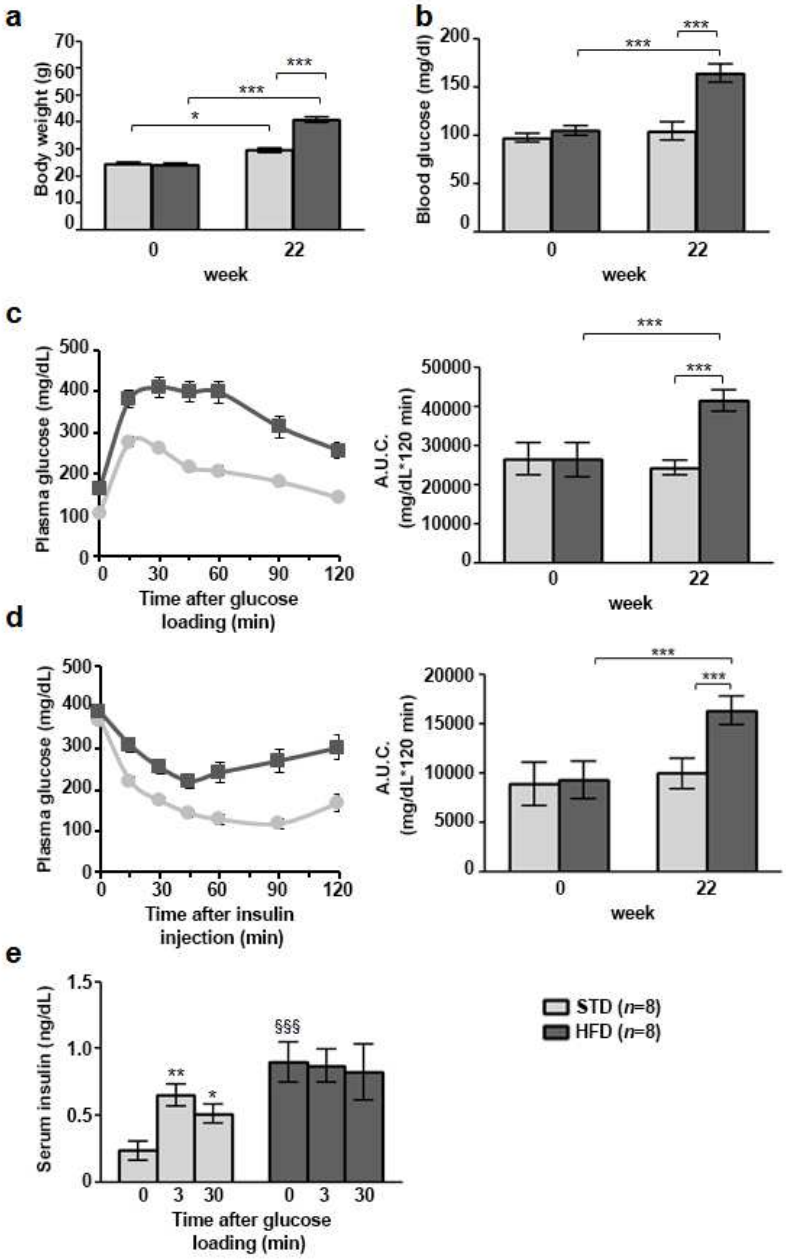

Figure 7 Effect of HFD on (a) Body weight, (b) fasting blood glucose, (c) glucose tolerance, (d) insulin sensitivity, (e) glucose stimulated insulin secretion. Data shown are mean ± SEM. Significant differences are indicated. *p<0.05, **p<0.01, *p<0.001. STD, standard diet; HFD, high fat diet; AUC, area under the curve.

Table 3 Biochemical parameters of C57Bl6/J mice fed with STD or HFD

weeks	0		22	
	STD	**HFD**	**STD**	**HFD**
CHOL (mg/dL)	95,2 ± 7,2	102,2 ± 8,3	97,7 ± 7,9	204,1 ± 8,9***,§§§
TG (mg/dL)	100,3 ± 9,7	99,7 ± 12,9	99,6 ± 11,5	116,5 ± 10,0
HDL (mg/dL)	54,8 ± 5,9	60,8 ± 5,02	54,2 ± 4,3	87,2 ± 2,4***,§§
LDL (mg/dL)	7,7 ± 1,3	6,6 ± 1,7	8,4 ± 0,9	17,9 ± 1,2***,§§§

Data are mean ± SEM of 8 animals/group. Total Cholesterol (CHOL), serum triglyceride (TG), serum HDL and LDL were determined in overnight fasted mice on high fat diet (HFD) or standard diet (STD) at the beginning and after 22 weeks of feeding. HFD *vs* STD at 22 weeks: $^{***}p<0.001$; HFD at 22 weeks *vs* HFD at 0 week: $^{§§§}p<0.001$.

4.3 Effect of high fat diet on Ped/Pea-15 levels in insulin target tissues

As I mentioned before, Phosphoprotein Enriched in Diabetes/ Phosphoprotein Enriched in Astrocytes (*Ped/Pea-15*) gene is commonly over-expressed in type 2 diabetic individuals. In this context, I investigated whether *Ped/Pea-15* expression could be affected by external cues, in particular by a high fat diet administration.

Therefore, by immunoblotting analysis I compared the PED/PEA-15 protein levels in liver, skeletal muscle and visceral adipose tissues of mice fed with standard or high fat diet for 22 weeks. The results show that HFD mice have higher PED/PEA-15 protein levels than STD mice both in skeletal muscle and adipose tissues but not in the liver (Figure 8).

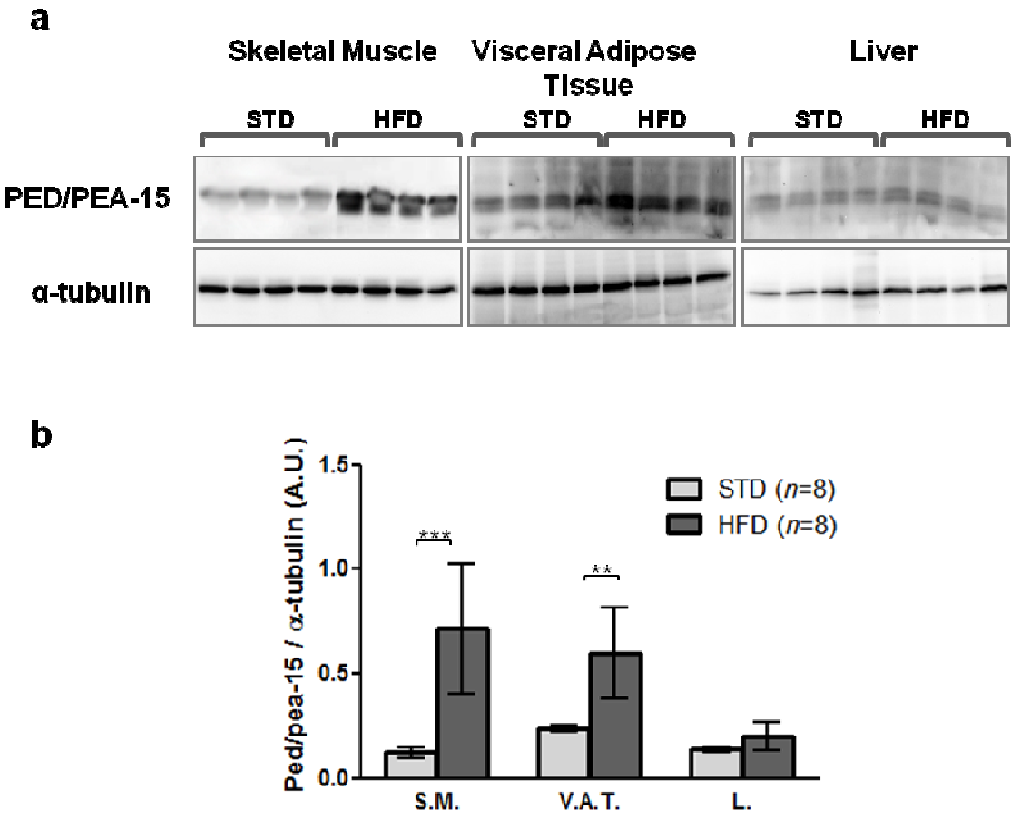

Figure 8 Ped/Pea-15 protein expression in insulin target tissues. a) Representative Western blot analysis of PED/PEA-15. Total protein extracts obtained from skeletal muscle (200μg.), visceral adipose tissue (50μg.) and liver (100μg) of C57Bl/6 mice fed a standard (STD) or high fat diet (HFD) for 22 weeks were separated by SDS-PAGE followed by immunoblotting with PED/PEA-15 antibody; alpha-tubulin was used as a loading control. **b)** Densitometric analyses of the data. Bars represent means ± SEM of 8 animals/group. S.M., skeletal muscle, V.A.T., visceral adipose tissue, L., liver. STD, standard diet; HFD, high fat diet. Asterisks denote statistically significant differences (**, $p<0.01$;***, $p<0.001$).

Consequently, to further investigate whether this increased expression is linked to a transcriptional regulation, I evaluated *Ped/Pea-15* mRNA expression by performing Real-time PCR (Figure 9). The results obtained confirmed western blot analysis. Indeed, the skeletal muscle and adipose tissues of HFD mice show three-fold and more than two-fold increase compared to control mice, respectively. Moreover, real time analysis suggest that *Ped/Pea-15* expression levels are higher in the liver than in skeletal muscle, however this result is not confirmed by western blot, suggesting that a post-transcriptional regulation could probably occur.

In conclusion, high fat diet affects *Ped/Pea-15* expression at transcriptional levels and this regulation seems to be regulated in a tissue-specific manner.

Therefore, for the first time it has been demonstrated that *Ped/Pea-15* can be modulated by environmental cues.

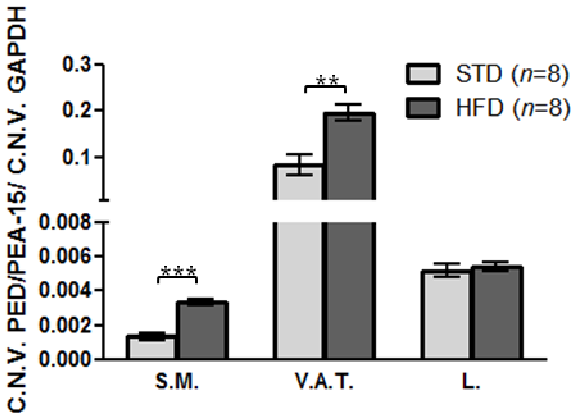

Figure 9 *Ped/Pea-15* mRNA expression levels in insulin target tissues. *Ped/Pea-15* mRNA levels were measured performing absolute cDNA quantification by Real-time PCR analysis. Data are shown as copy number variation (C.N.V.) of PED/PEA-15 normalized on CNV of a reference gene. Bars are means ± SEM of 8 animals/group. S.M., skeletal muscle, V.A.T., visceral adipose tissue, L., liver; STD, standard diet; HFD, high fat diet. Asterisks denote statistically significant differences (**, $p<0.01$;***, $p<0.001$).

4.4 Effect of high fat diet on chromatin remodelling at *PED/PEA-15* promoter

It is well demonstrated that the recruitment of transcription factors to their sequence targets may require chromatin-modifying events that, opening chromatin, allow access to the transcriptional machinery.

Therefore, I aimed to analyze the dynamics of chromatin organization at *Ped/Pea-15* promoter upon high fat diet administration. In particular, I performed Formaldehyde-Assisted Isolation of Regulatory Elements (FAIRE) assays on 2000 base pairs upstream *Ped/Pea-15* transcription start site, both in skeletal muscle and in liver of STD and HFD mice (Figure 10).

The results obtained in the skeletal muscle show an enrichment in the FAIRE signal in the region across the transcription start site. Interestingly, an increased signal is also detectable in the region ranging from -2000 to -1475 (Figure 10b). Enrichment of FAIRE signal denotes a more open structure of the chromatin. These results suggest that, at least in skeletal muscle tissue a nucleosomes reorganization is undergoing upon high fat diet treatment. In contrast, the region from -823 to 225 shows an opposite profile, resulting in a less open chromatin in HFD mice compared to control mice (Figure 10b).

FAIRE analysis performed in the liver revealed a quite different profile respect to that obtained in skeletal muscle (Figure 10c).

As shown in Figure 10c, FAIRE signals in the liver progressively increase from -823 to the transcription start site. However, not statistically differences were observed between STD and HFD mice, suggesting that fat-enriched diet does not exert any role in chromatin remodelling at *Ped/Pea-15* promoter in the liver. In addition, the region ranging from -2000 to -1475 showed a very low FAIRE signal (Fig.10c). This appeared as the strongest difference between the two tissues examined.

Thus, all together these data suggest that the higher *Ped/Pea-15* expression levels observed in muscle, upon high fat diet administration, may correlate with chromatin reorganization observed in the FAIRE assays.

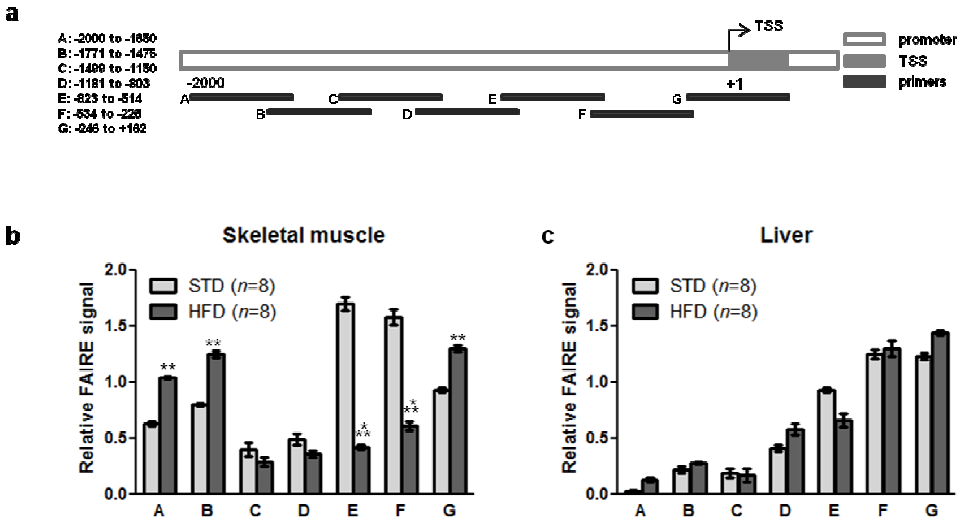

Figure 10 Chromatin remodelling response upon high fat diet administration. a) Schematic representation of *Ped/Pea-15* promoter region; black bars indicate regions analyzed by Formaldehyde Assisted Isolation of Regulatory Elements, amplified with seven different primers pairs (listed in Table 2) by semiquantitative PCR. **b-c)** FAIRE analysis was performed both in muscle and liver, of STD and HFD mice. FAIRE signals were normalized to INPUT control. Bars are means ± SEM of 8 animals/group. Regions that demonstrated less than 20% of induction upon high fat diet were classified as non responsive. TSS, transcription start site; STD, standard diet; HFD, high fat diet. Asterisks denote statistically significant differences (**, $p<0.01$;***, $p<0.001$).

4.5 Effect of high fat diet on nucleosomes positioning at the *Ped/Pea-15* promoter

To clarify whether the increase in the FAIRE signals observed at specific *Ped/Pea-15* regions were a direct consequence of nucleosomes removal, I performed Micrococcal Nuclease (MNase) assays.

Many studies indicated that nucleosome organization is somewhat nonrandom and that some regions of the genome are more likely to contain nucleosomes than others. Thus, nucleosomes positioning has clear implications for gene regulation.

After nuclei isolation and MNase digestion, nucleosome-protected DNA was evaluated by qPCR and data are represented as the percentage of the loss of amplification following MNase digestion. As shown in Figure 11, the amount of nucleosome-bound DNA in STD and HFD mice, both in the skeletal muscle and in the liver, is lower around the transcription start site (region G) compared to the upstream fragments analyzed (regions A-B), as expected. Indeed, open promoters regulating the expression of constitutive genes, generally lack nucleosomes at transcription start site allowing access to transcription factors. Interestingly, in the skeletal muscle of HFD mice regions that demonstrated increased FAIRE signals (regions A-B) showed increased MNase sensitivity, reported as reduced nucleosome-bound DNA, thus suggesting a more open chromatin compared to their control mice (Figure 11).

At variance, in the liver high fat diet did not affect chromatin structure at the same regions, confirming FAIRE results previously obtained (Figure 11). Moreover, since the increased MNase sensitivity observed in the regions A and B of HFD mice skeletal muscle is not so strong as that obtained in region G, it could reflect a more active chromatin conformation rather than nucleosome depleted regions.

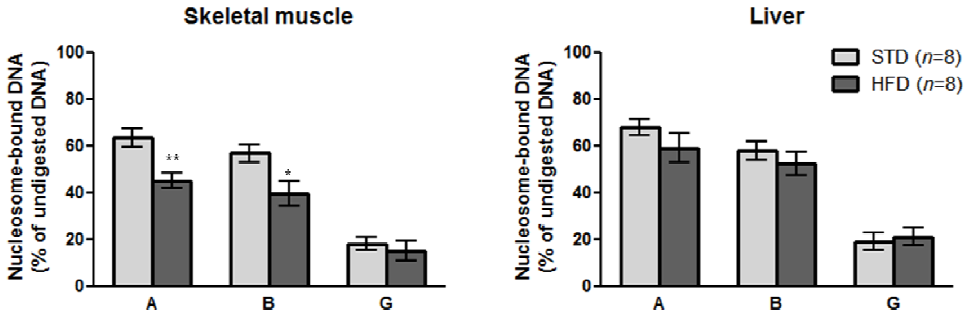

Figure 11 Micrococcal Nuclease (MNase) assays upon high fat diet administration. MNase analysis was performed both in muscle and liver, of STD and HFD mice after 22 weeks of feeding. After MNase digestion, nucleosome-bound DNA was analyzed by qPCR and normalized to not digested DNA. Bars are means ± SEM of 8 animals/group. STD, standard diet; HFD, high fat diet; A: from -2000 to -1650; B: from -1771 to -1475; G: from –245 to +162 (distance are relative to Ped/Pea-15 transcription start site). Asterisks denote statistically significant differences (*, $p<0.01$**, $p<0.01$).

To better address this point, I decided to perform chromatin immunoprecipitation assays using an antibody against histone H3 in order to evaluate the presence or absence of nucleosome structures.

Regions that showed significant increase in FAIRE signals did not result in increased nucleosomes depletion in HFD mice compared to control mice (Figure 12). Moreover, not significant differences were observed between skeletal muscle and liver. Indeed, in both tissues, the region across the transcription start site (TSS) (region G) showed a very low signal compared to the other regions analyzed (region A-B), in concordance with the principle of nucleosomes depletion at TSSs.

Therefore, overall these data suggest a general constant nucleosome residency with changes in chromatin architecture.

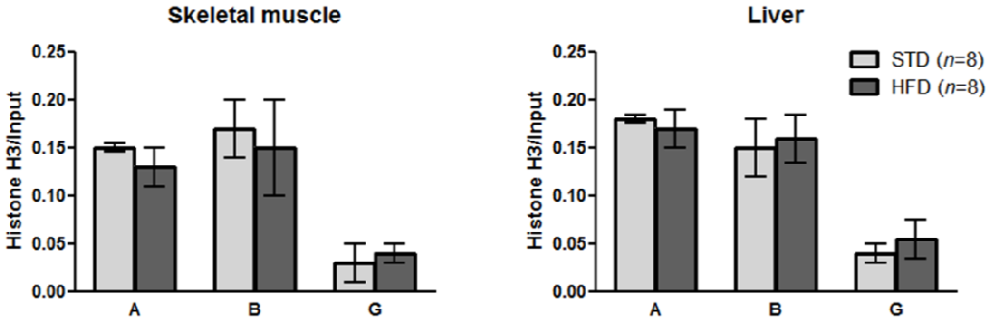

Figure 12 Nucleosome occupancy at *Ped/Pea-15* promoter. Relative quantification of total histone H3 antibody at specific Ped/Pea-15 promoter, in skeletal muscle and liver (left and right panels, respectively). Data are normalized to Input control and are means ± SEM of 8 animals/group. STD, standard diet; HFD, high fat diet; A: from -2000 to -1650; B: from -1771 to -1475; G: from –245 to +162 (distance are relative to Ped/Pea-15 transcription start site).

4.6 Effect of high fat diet on histone modification at Ped/Pea-15 promoter

Gene transcription and activation are dynamic processes involving the conversion of more closed chromatin into transcription factor-accessible euchromatin (Berger, 2007). A key role in these processes is played by histone modifications. Their presence or absence may create or disrupt chromatin contacts. Among the modifications of different histones, those on histones H3 and H4 are the most studied and involved in the regulation of gene expression (Grunstein, 1997; Lachner & Jenuwein, 2002). Moreover, regulation of histone modifications has been shown to be influenced by nutrients (Wellen et al, 2009; Wheatley et al, 2011).

Therefore, I hypothesized that increased *Ped/Pea-15* expression in the skeletal muscle tissue of HFD mice may be the results of specific histone modifications, occurring at its promoter, associated to active gene transcription.

To test this hypothesis, I evaluated the levels of histone 4 acetylation (AcH4) and di-methylation of lysine 4 on histone 3 (H3K4me2) that commonly dictate gene activation, and di-methylation of lysine 9 on histone 3 (H3K9me2) a marker of gene repression. These histone marks were globally evaluated on the promoter region covering 2000 base pairs upstream the transcription start site (TSS) of *Ped/Pea-15* gene (Figure 13). Chromatin immunoprecipitation analysis show that both AcH4 and H3K4me2 are increased in the skeletal muscle tissue but not in the liver upon 22 weeks of high fat diet administration. In contrast, H3K9me2 levels were low in both tissues and no differences between the two groups of animals were detected. These results suggest that

increasing levels of *Ped/Pea-15* gene in skeletal muscle tissue are also accompanied by an increase of euchromatin histone marks.

In contrast, in the liver, in which the gene does not increase upon high fat diet administration, any increase is detected. All together these data suggest a possible correlation between high fat diet induced histone modifications and gene expression.

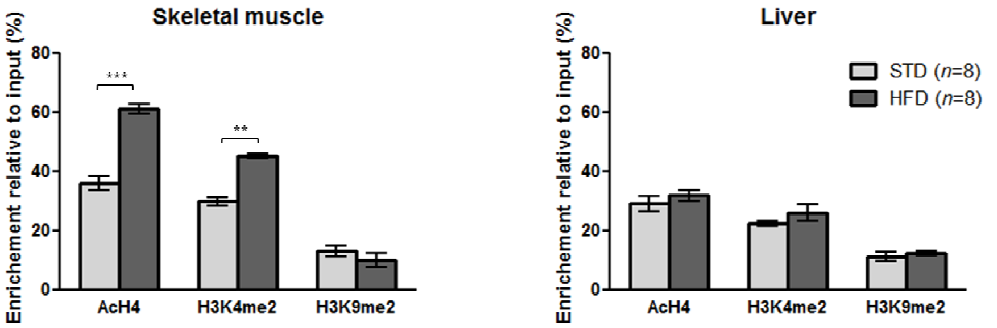

Figure 13 High fat diet increases histone H4 acetylation and lysine 4 di-methylation at PED/PEA-15 promoter. Relative quantification of *Ped/Pea-15* promoter region DNA immunoprecipitated with anti -AcH4, -H3K4me2 and -H3K9me2 antibodies, in skeletal muscle and liver of STD and HFD mice (left and right panels, respectively). Chromatin immunoprecipitation was followed by PCR amplification with primers spanning the 2000 base pairs upstream the Ped/PEA-15 transcription start site. Results are expressed as enrichment relative to input (%) and corrected for IgG control levels. Data are means ± SEM of 8 animals/group. AcH4, acetyl histone H4; H3K4me2, di-methyl lysine 4 on histone H3; H3K9me2, di-methyl lysine 9 on histone H3; STD, standard diet; HFD, high fat diet. Asterisks denote statistically significant differences (**, $p<0.01$;***, $p<0.001$).

Thus, to get further insight into the functional role of AcH4 and H3K4me2 in the regulation of *Ped/Pea-15* expression, I performed a chromatin immunoprecipitation-walking to identify the enrichment of these histone marks at specific regions of *Ped/Pea-15* promoter (Figure 14). Comparing relative abundance of histone modifications, histone 4 acetylation is markedly increased in skeletal muscle of HFD mice compared to control mice. In particular, acetylation increases in proximity of the transcription start site; interestingly, in the region from -2000 to -1475 it shows the highest levels (Figure 14b). In contrast, acetylation levels in liver of HFD mice slight increase nearby the transcription start site and never reach the levels recorded in skeletal muscle. Moreover, any increase of AcH4 have been detected around -2000 bp (regions A-B) in the liver upon high fat diet administration (Figure 14c). In parallel, H3K4me2 levels increases in the muscle but not in the liver upon high fat diet administration (Figure 14 d-e). However it has not been detected a strong increase as acetylation. Finally, no differences were observed regarding

H3K9me2 levels between the two experimental groups, in both tissues, suggesting that this histone mark does probably not play any role in the regulation of PED/PEA-15 gene (Figure 14 f-g).

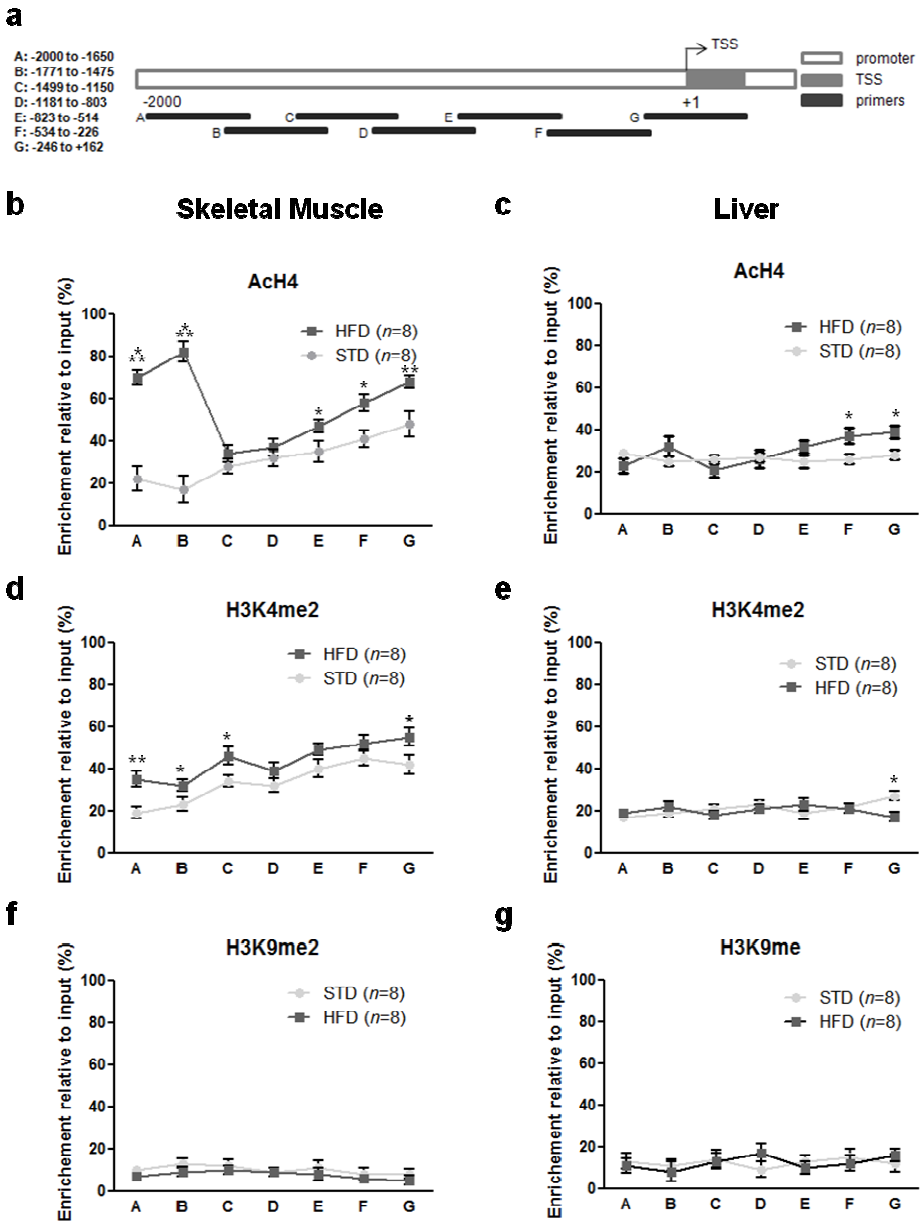

Figure 14 Relative abundance of histone modifications on PED/PEA-15 promoter. a) Schematic representation of *Ped/Pea-15* promoter; black bars indicate regions analyzed by Chromatin immunoprecipitation assays and amplified by seven different primers pairs (listed in Table 2) spanning the 2000 base pairs upstream the Ped/PEA-15 transcription start site. distances are relative to transcription start site. **b-g)** Plots show the AcH4, H3K4me2 and H3K9me2 levels on Ped/Pea-15 promoter in skeletal muscle (left panels) and in liver (right panels). Results are expressed as enrichment relative to input (%) and corrected for IgG control levels. Data are means ± SEM of 8 animals/ group. STD, standard diet; HFD, high fat diet. Asterisks denote statistically significant differences (*, $p<0.05$; **, $p<0.01$;***, $p<0.001$).

4.7 Tissue-specific effect of high fat diet on a distal *Ped/pea-15* promoter region

It is now clear that non-coding sequences play a key role in regulating gene expression. Moreover, transcription can be regulated by multiple and different types of *cis*-regulatory elements that can also act over distance. Distant regulatory elements, such as enhancers, have the ability to regulate tissue-specific gene expression in an orientation dependent manner (Jin et al, 2011).

With respect to enhancer identification, a particularly relevant insight was the identification of specific histone methylation signatures. In contrast to promoters, which are marked by trimethylation of histone H3 at lysine residue 4 (H3K4me3), active enhancers are characterized by monomethylation at the same position (H3K4me1) (Visel et al, 2009). In addition, based on the presence/absence of histone acetylation they can be classified into active or poised enhancers, respectively (Creyghton et al, 2010; Rada-Iglesias et al, 2011). Importantly, these predicted enhancers can be also frequently associated with co-activators like p300 or TRAP220.

Based on this knowledge, I wondered whether the distal promoter region analyzed could act as a distal regulatory element. Therefore, I performed chromatin immunoprecipitation assays in order to evaluate the levels of monomethylated lysine 4 at histone H3 (H3K4me1). As shown in Figure 15a, H3K4me1 levels strongly increase upon high fat diet administration in skeletal muscle tissue but not in the liver. Moreover, mice fed standard diet show higher levels of H3K4me1 in muscle than in liver ($p<0.05$), suggesting that this region could have a role in skeletal muscle but not in the liver in regulating *Ped/Pea-15* expression.

As discussed above, distal regulatory regions can be classified into "poised" or "active" based on their acetylation levels. In particular, poised enhancers are associated with basal levels of H3K4me1 without H3K27Ac. Thus, upon appropriate stimulations they can switch from poised to active enhancers, acquiring H3K27Ac (Ostuni et al, 2013). Therefore, I evaluated H3K27Ac levels and, as shown in Figure 15a, the monomethylation of lysine 4 is accompanied by the acetylation at lysine residue 27 in the skeletal muscle of high fed diet mice, whereas the same region in the liver does not acquire this feature.

Then, I also evaluated the trimethylation levels at lysine residue 4 on histone H3 (Figure 15b). This histone mark is enriched at active promoter regions. Chromatin immunoprecipitation experiments revealed that H3K4me3 levels can be detected across PED/PEA-15 transcription start site both in muscle and in liver, indicating that the gene is transcribed in both tissues. Moreover, upon

high fat diet administration H3K4me3 levels result in a slight increase in the liver and in a much more consistent increase in skeletal muscle. Finally, I considered an additional feature known to be associated with promoters, that is RNA polymerase II. The recruitment of RNA polymerase II is detectable in the two experimental groups in skeletal muscle as well as in the liver. However, there is an increase in its recruitment only in the muscle upon high fat diet administration (Figure 15b).

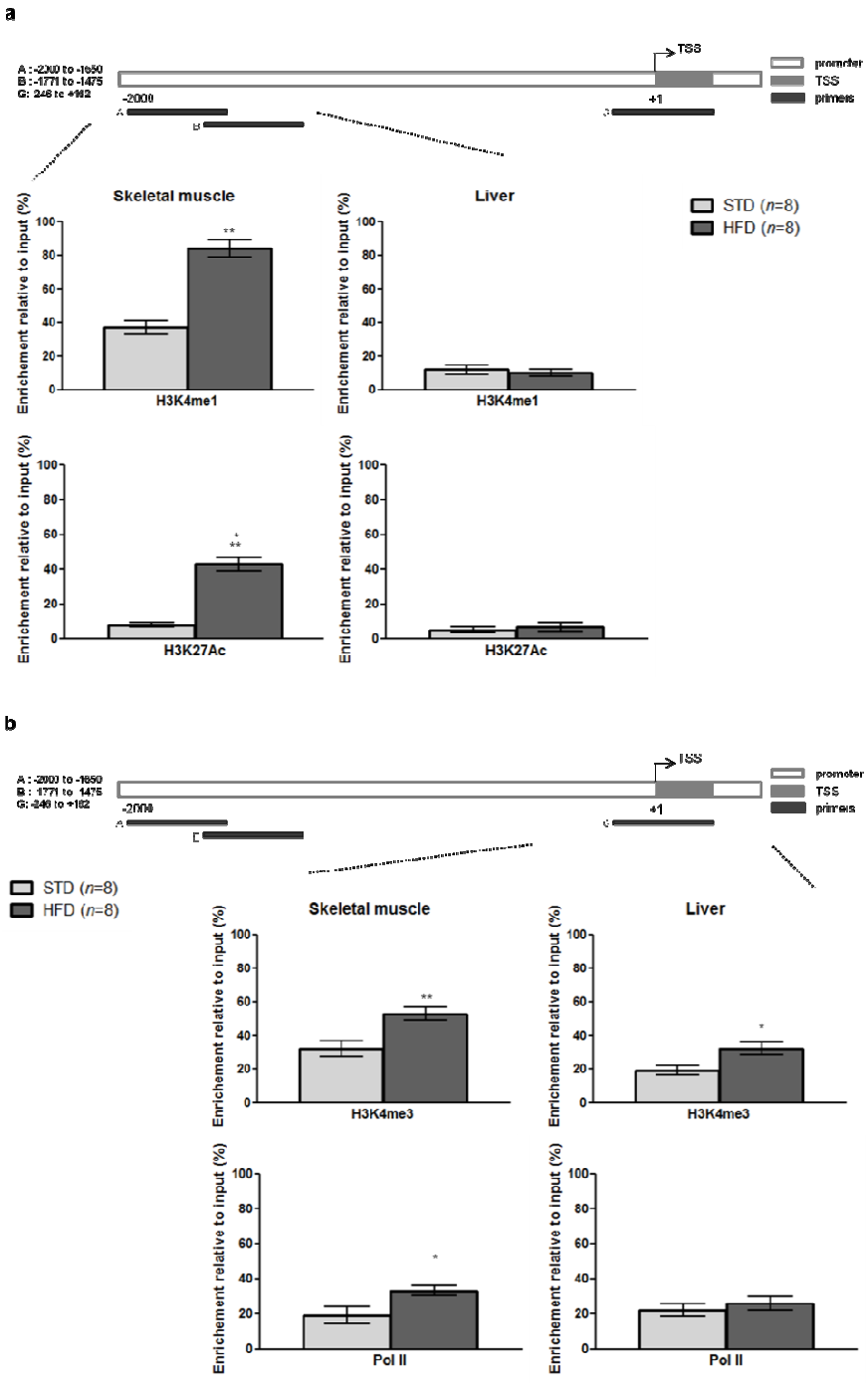

Figure 15 Specific histone marks enrichment at selected *Ped/Pea-15* promoter regions. ChIP experiments were performed using antibodies against H3K4me1, H3K27Ac, H3K4me3 and Pol II or nonspecific IgG antibodies. Chromatin immunoprecipitation was followed by PCR amplification with primers for A, B and G regions as indicated in theschematic representation of *Ped/Pea-15* promoter **a)** Bar graphs show H3K4me1 and H3K27Ac levels on distal promoter region (from -2000 to -1475). **b)**. Bar graphs show H3K4me3 levels and Pol II recruitment across *Ped/Pea-*

15 TSS (-246 to +162). Results are expressed as enrichment relative to input (%), corrected for IgG control levels and are means ± SEM of 8 animals/ group. H3K4me1, monomethylation of lysine 4 on histone H3; H3K27Ac, acetylation of lysine 27 on histone H3; H3K4me3, trimethylation of lysine 4 on histone H3; Pol II, Polymerase II; TSS, transcription start site. STD, standard diet; HFD, high fat diet. Asterisks denote statistically significant differences (*, $p<0.05$; **, $p<0.01$;***, $p<0.001$).

Different classes of histone methyltransferase can mediate the H3K4me1: the SET-domain containing protein, the ASH-like protein and the MLL-proteins. It has been recently demonstrated that SET7/9 may regulate gene expression under hyperglycaemic/hyperinsulinemic conditions and it is involved in the development and in the progression of diabetic vascular complications.

Thus, I wanted to determine whether SET7/9 is involved in the monomethylation of *Ped/Pea-15* promoter. Therefore, I performed chromatin immunoprecipitation assay using antibody against SET7/9 followed by the amplification of regions that showed higher levels of H3K4me1(regions A-B) (Figure 16). As shown in figure 16a, SET7/9 binds *Ped/Pea-15* promoter even though there is no further recruitment in the skeletal muscle tissue upon high fat diet administration. Although I observed an increase in histone H3K4 monomethylation in the skeletal muscle, the binding of SET7/9 enzyme was not changed. This result could be explained in different ways; it is possible that high fat diet may alter its enzymatic activity rather than its amount at the selected promoter region. Moreover, SET7/9 is not the only histone methyltransferase that mediates this modification and thus it is possible that other enzymes take part to this process. Instead, in the liver low levels of H3K4me1 well correlate with low levels of SET7/9 at Ped/Pea-15 promoter, both in high fat diet and standard mice (Figure 16b).

In addition, because distal regulatory elements can be associated with the histone acetyltransferase p300, I also tested its recruitment at Ped/Pea-15 promoter region associated with high levels of acetylated H3K27 (Figure 16). Upon high fat diet administration, the binding of p300 in the skeletal muscle strongly increased compared to standard mice (Figure 16a). At variance, this increase was not observed in the liver (Figure 16b).

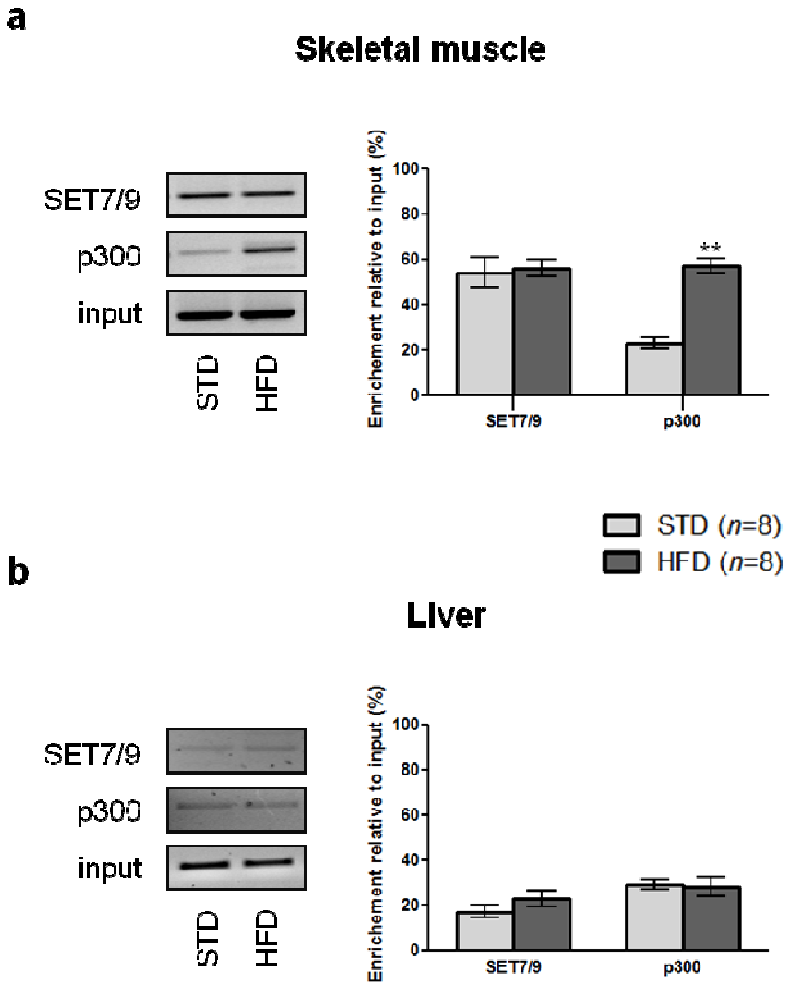

Figure 16 SET7/9 and p300 recruitment at the Ped/Pea-15 promoter. Cromatin immunoprecipitation assays were performed using antibodies against SET7/9 and p300. ChIP-enriched samples were amplified by semiquantitative PCR using specific *Ped/Pea15* promoter primers amplifying regions A (from -2000 to -1650) and B (from -1771 to -1475). Experiments were performed in skeletal muscle **(a)** and in liver **(b)**. Bar graphs are means ± SEM of 8 animals/ group and are expressed as enrichment relative to input (%), corrected for IgG control levels. STD, standard diet; HFD, high fat diet. Asterisks denote statistically significant differences (**, $p<0.01$).

In the last years enhancer have attracted much attention due to their ability and critical role in regulating gene expression. Active enhancers may activate genes trough different mechanisms, such as direct interaction with promoter, altering nuclear organization, changing chromatin structure. Thus, all together these data suggest that this distant region could be responsible of the tissue-specific *Ped/Pea-15* up-regulation upon high fat diet administration. Studies in the shape of the genome provided evidence that distal regulatory DNA

sequences can control transcription over distance by physically contacting target genes via chromatin looping (Holwerda & de Laat, 2012). It would be a great challenge to demonstrate that this mechanism also occur on *Ped/Pea-15* promoter. Thereby run-on experiments aims at evaluating the physical contact between this distal region and the proximal promoter through chromatin conformation capture technique (3C).

5. CONCLUSIONS

This work has identified the impact of the environment on the regulation of *Ped/Pea-15* gene focusing on chromatin modification phenomena. The administration of a high fat diet in mice is able to affect *Ped/Pea-15* expression in insulin target tissues, through transcriptional regulation. Indeed, its transcriptional levels increased in skeletal muscle and in visceral adipose tissue but not in the liver, thus suggesting potential tissue-specific mechanisms.

Moreover, the increased expression was accompanied by a change of chromatin organization not due to a nucleosomes repositioning but to a change in histone modifications. Specifically, *Ped/Pea-15* levels increase together with histone 4 acetylation and histone 3 dimethylation at lysine 4 on its promoter region. These two histone marks are associated with active chromatin and therefore may be involved in the regulation of *Ped/Pea-15* mRNA expression.

This study also provides new insight regarding the presence of a distal regulatory element switched from poised into active *status* upon high fat diet administration that can have an impact on chromatin organization and transcriptional activity of the gene.

Since evidence linking specific environmental cues and metabolic disorders are still limited, elucidating the mechanisms through which environmental factors can alter metabolic homeostasis remain a challenge.

Phosphoprotein Enriched in Diabetes/Phosphoprotein enriched in Astrocytes (PED/PEA-15) gene plays a crucial role in the regulation of insulin sensitivity, both in humans and in rodents. Indeed, the overexpression of this gene is a common feature of type 2 diabetic individuals.

Therefore highlighting how environment impacts on its expression could be a good-model to understand more general epigenetic mechanisms by which nutrition interacts with the genome thereby influencing metabolic health.

6. ACKNOWLEDGEMENTS

I would like to thank Professor Pietro Formisano for his helpful teaching activity as my tutor during my PhD.

I would like to thank Professor Francesco Beguinot, who gave me the opportunity to be part of his working group.

I would like to express my gratitude to my direct supervisor, Dr. Paola Ungaro. She always encouraged and helped me to shape my interest and ideas.

My sincere thanks also goes to Professor Beato, for gave me the opportunity to join his research group at the Centre for Genomic Regulation, as a visiting PhD student. In particular, I would like to thank Dr Roni Wright for teaching me so much in so few time.

I am also indebted to the students I had the pleasure to work with. Thanks to Sara and Rosaria, who were involved in this project. They were a great help in running the experiments, they were responsible and cooperative with solving the problems. I sincerely thank Rosaria, who even after her graduation decided to help me in these last critical months.

I would also like to thank all the people of the lab, from "Edificio 4" to "Corpi Bassi", for our exchanges of knowledge, skills, time spent together, and venting of frustration during my graduate program. Particularly, special thanks to Carmela, who has been *a friend* giving me her support when I have needed it the most.

I would also like to thank my family: my mother, my father and my aunt for always believing in me, for their continuous love and, above all, for their supports in my decisions.

I *must* acknowledge Giuseppe, partner in life and work. I could not have completed this thesis without him by my side. He went through every excruciating step and mood change with me. His wit has kept me smiling and gave me a different view of the world that has helped keep things in perspective. Thank you because you motivated me in so many ways.

7. REFERENCES

Araujo H, Danziger N, Cordier J, Glowinski J, Chneiweiss H (1993) Characterization of PEA-15, a major substrate for protein kinase C in astrocytes. *The Journal of biological chemistry* **268:** 5911-5920

Bandyopadhyay GK, Yu JG, Ofrecio J, Olefsky JM (2005) Increased p85/55/50 expression and decreased phosphotidylinositol 3-kinase activity in insulin-resistant human skeletal muscle. *Diabetes* **54:** 2351-2359

Bannister AJ, Kouzarides T (2005) Reversing histone methylation. *Nature* **436:** 1103-1106

Barroso I (2005) Genetics of Type 2 diabetes. *Diabetic medicine : a journal of the British Diabetic Association* **22:** 517-535

Berger SL (2007) The complex language of chromatin regulation during transcription. *Nature* **447:** 407-412

Buhman KK, Accad M, Novak S, Choi RS, Wong JS, Hamilton RL, Turley S, Farese RV, Jr. (2000) Resistance to diet-induced hypercholesterolemia and gallstone formation in ACAT2-deficient mice. *Nature medicine* **6:** 1341-1347

Callaway K, Abramczyk O, Martin L, Dalby KN (2007) The anti-apoptotic protein PEA-15 is a tight binding inhibitor of ERK1 and ERK2, which blocks docking interactions at the D-recruitment site. *Biochemistry* **46:** 9187-9198

Choudhuri S (2011) From Waddington's epigenetic landscape to small noncoding RNA: some important milestones in the history of epigenetics research. *Toxicology mechanisms and methods* **21:** 252-274

Condorelli G, Trencia A, Vigliotta G, Perfetti A, Goglia U, Cassese A, Musti AM, Miele C, Santopietro S, Formisano P, Beguinot F (2002) Multiple members of the mitogen-activated protein kinase family are necessary for PED/PEA-15 anti-apoptotic function. *The Journal of biological chemistry* **277:** 11013-11018

Condorelli G, Vigliotta G, Cafieri A, Trencia A, Andalo P, Oriente F, Miele C, Caruso M, Formisano P, Beguinot F (1999) PED/PEA-15: an anti-apoptotic molecule that regulates FAS/TNFR1-induced apoptosis. *Oncogene* **18:** 4409-4415

Condorelli G, Vigliotta G, Iavarone C, Caruso M, Tocchetti CG, Andreozzi F, Cafieri A, Tecce MF, Formisano P, Beguinot L, Beguinot F (1998) PED/PEA-15 gene controls glucose transport and is overexpressed in type 2 diabetes mellitus. *The EMBO journal* **17:** 3858-3866

Condorelli G, Vigliotta G, Trencia A, Maitan MA, Caruso M, Miele C, Oriente F, Santopietro S, Formisano P, Beguinot F (2001) Protein kinase C (PKC)-alpha activation inhibits PKC-zeta and mediates the action of PED/PEA-15 on glucose transport in the L6 skeletal muscle cells. *Diabetes* **50:** 1244-1252

Creyghton MP, Cheng AW, Welstead GG, Kooistra T, Carey BW, Steine EJ, Hanna J, Lodato MA, Frampton GM, Sharp PA, Boyer LA, Young RA, Jaenisch R (2010) Histone H3K27ac separates active from poised enhancers and predicts developmental state. *Proceedings of the National Academy of Sciences of the United States of America* **107:** 21931-21936

Danziger N, Yokoyama M, Jay T, Cordier J, Glowinski J, Chneiweiss H (1995) Cellular expression, developmental regulation, and phylogenic conservation of PEA-15, the astrocytic major phosphoprotein and protein kinase C substrate. *Journal of neurochemistry* **64:** 1016-1025

de Groote ML, Verschure PJ, Rots MG (2012) Epigenetic Editing: targeted rewriting of epigenetic marks to modulate expression of selected target genes. *Nucleic acids research* **40:** 10596-10613

Dhanasekaran S, Doherty TM, Kenneth J, Group TBTS (2010) Comparison of different standards for real-time PCR-based absolute quantification. *Journal of immunological methods* **354:** 34-39

Feige JN, Auwerx J (2007) Transcriptional coregulators in the control of energy homeostasis. *Trends in cell biology* **17:** 292-301

Formstecher E, Ramos JW, Fauquet M, Calderwood DA, Hsieh JC, Canton B, Nguyen XT, Barnier JV, Camonis J, Ginsberg MH, Chneiweiss H (2001) PEA-15 mediates cytoplasmic sequestration of ERK MAP kinase. *Developmental cell* **1:** 239-250

Gaumont-Leclerc MF, Mukhopadhyay UK, Goumard S, Ferbeyre G (2004) PEA-15 is inhibited by adenovirus E1A and plays a role in ERK nuclear export and Ras-induced senescence. *The Journal of biological chemistry* **279:** 46802-46809

Greer EL, Shi Y (2012) Histone methylation: a dynamic mark in health, disease and inheritance. *Nature reviews Genetics* **13:** 343-357

Grunstein M (1997) Histone acetylation in chromatin structure and transcription. *Nature* **389:** 349-352

Haberland M, Montgomery RL, Olson EN (2009) The many roles of histone deacetylases in development and physiology: implications for disease and therapy. *Nature reviews Genetics* **10:** 32-42

Hao C, Beguinot F, Condorelli G, Trencia A, Van Meir EG, Yong VW, Parney IF, Roa WH, Petruk KC (2001) Induction and intracellular regulation of tumor necrosis factor-related apoptosis-inducing ligand (TRAIL) mediated apotosis in human malignant glioma cells. *Cancer research* **61:** 1162-1170

Hayhurst GP, Lee YH, Lambert G, Ward JM, Gonzalez FJ (2001) Hepatocyte nuclear factor 4alpha (nuclear receptor 2A1) is essential for maintenance of hepatic gene expression and lipid homeostasis. *Molecular and cellular biology* **21:** 1393-1403

Holwerda S, de Laat W (2012) Chromatin loops, gene positioning, and gene expression. *Frontiers in genetics* **3:** 217

Hwang S, Kuo WL, Cochran JF, Guzman RC, Tsukamoto T, Bandyopadhyay G, Myambo K, Collins CC (1997) Assignment of HMAT1, the human homolog of the murine mammary transforming gene (MAT1) associated with tumorigenesis, to 1q21.1, a region frequently gained in human breast cancers. *Genomics* **42:** 540-542

Itani SI, Ruderman NB, Schmieder F, Boden G (2002) Lipid-induced insulin resistance in human muscle is associated with changes in diacylglycerol, protein kinase C, and IkappaB-alpha. *Diabetes* **51:** 2005-2011

Jaenisch R, Bird A (2003) Epigenetic regulation of gene expression: how the genome integrates intrinsic and environmental signals. *Nature genetics* **33 Suppl:** 245-254

Jin F, Li Y, Ren B, Natarajan R (2011) Enhancers: multi-dimensional signal integrators. *Transcription* **2:** 226-230

Kawaji H, Nakamura M, Takahashi Y, Sandelin A, Katayama S, Fukuda S, Daub CO, Kai C, Kawai J, Yasuda J, Carninci P, Hayashizaki Y (2008) Hidden layers of human small RNAs. *BMC genomics* **9:** 157

Kirk EA, Moe GL, Caldwell MT, Lernmark JA, Wilson DL, LeBoeuf RC (1995) Hyper- and hypo-responsiveness to dietary fat and cholesterol among inbred mice: searching for level and variability genes. *Journal of lipid research* **36:** 1522-1532

Kouzarides T (2007) Chromatin modifications and their function. *Cell* **128:** 693-705

Lachner M, Jenuwein T (2002) The many faces of histone lysine methylation. *Current opinion in cell biology* **14:** 286-298

Latham JA, Dent SY (2007) Cross-regulation of histone modifications. *Nature structural & molecular biology* **14:** 1017-1024

Lee DY, Teyssier C, Strahl BD, Stallcup MR (2005) Role of protein methylation in regulation of transcription. *Endocrine reviews* **26:** 147-170

Lin HV, Accili D (2011) Hormonal regulation of hepatic glucose production in health and disease. *Cell metabolism* **14:** 9-19

Liu CL, Kaplan T, Kim M, Buratowski S, Schreiber SL, Friedman N, Rando OJ (2005) Single-nucleosome mapping of histone modifications in S. cerevisiae. *PLoS biology* **3:** e328

Maunakea AK, Nagarajan RP, Bilenky M, Ballinger TJ, D'Souza C, Fouse SD, Johnson BE, Hong C, Nielsen C, Zhao Y, Turecki G, Delaney A, Varhol R, Thiessen N, Shchors K, Heine VM, Rowitch DH, Xing X, Fiore C, Schillebeeckx M, Jones SJ, Haussler D, Marra MA, Hirst M, Wang T, Costello JF (2010) Conserved role of intragenic DNA methylation in regulating alternative promoters. *Nature* **466:** 253-257

Miele C, Raciti GA, Cassese A, Romano C, Giacco F, Oriente F, Paturzo F, Andreozzi F, Zabatta A, Troncone G, Bosch F, Pujol A, Chneiweiss H, Formisano P, Beguinot F (2007) PED/PEA-15 regulates glucose-induced insulin secretion by restraining potassium channel expression in pancreatic beta-cells. *Diabetes* **56:** 622-633

Morris KV (2009) Non-coding RNAs, epigenetic memory and the passage of information to progeny. *RNA biology* **6:** 242-247

Osborn O, Olefsky JM (2012) The cellular and signaling networks linking the immune system and metabolism in disease. *Nature medicine* **18:** 363-374

Ostuni R, Piccolo V, Barozzi I, Polletti S, Termanini A, Bonifacio S, Curina A, Prosperini E, Ghisletti S, Natoli G (2013) Latent enhancers activated by stimulation in differentiated cells. *Cell* **152:** 157-171

Patel CJ, Bhattacharya J, Butte AJ (2010) An Environment-Wide Association Study (EWAS) on type 2 diabetes mellitus. *PloS one* **5:** e10746

Peacock JW, Palmer J, Fink D, Ip S, Pietras EM, Mui AL, Chung SW, Gleave ME, Cox ME, Parsons R, Peter ME, Ong CJ (2009) PTEN loss promotes mitochondrially dependent type II Fas-induced apoptosis via PEA-15. *Molecular and cellular biology* **29:** 1222-1234

Pereira FA, Tsai MJ, Tsai SY (2000) COUP-TF orphan nuclear receptors in development and differentiation. *Cellular and molecular life sciences : CMLS* **57:** 1388-1398

Pokholok DK, Harbison CT, Levine S, Cole M, Hannett NM, Lee TI, Bell GW, Walker K, Rolfe PA, Herbolsheimer E, Zeitlinger J, Lewitter F, Gifford DK, Young RA (2005) Genome-wide map of nucleosome acetylation and methylation in yeast. *Cell* **122:** 517-527

Rada-Iglesias A, Bajpai R, Swigut T, Brugmann SA, Flynn RA, Wysocka J (2011) A unique chromatin signature uncovers early developmental enhancers in humans. *Nature* **470:** 279-283

Rassoulzadegan M, Grandjean V, Gounon P, Vincent S, Gillot I, Cuzin F (2006) RNA-mediated non-mendelian inheritance of an epigenetic change in the mouse. *Nature* **441:** 469-474

Rossetto D, Avvakumov N, Cote J (2012) Histone phosphorylation: a chromatin modification involved in diverse nuclear events. *Epigenetics : official journal of the DNA Methylation Society* **7:** 1098-1108

Sanghera DK, Blackett PR (2012) Type 2 Diabetes Genetics: Beyond GWAS. *Journal of diabetes & metabolism* **3**

Schwer B, Verdin E (2008) Conserved metabolic regulatory functions of sirtuins. *Cell metabolism* **7:** 104-112

Seino S, Shibasaki T, Minami K (2011) Dynamics of insulin secretion and the clinical implications for obesity and diabetes. *The Journal of clinical investigation* **121:** 2118-2125

Shi Y, Lan F, Matson C, Mulligan P, Whetstine JR, Cole PA, Casero RA, Shi Y (2004) Histone demethylation mediated by the nuclear amine oxidase homolog LSD1. *Cell* **119:** 941-953

Shogren-Knaak M, Ishii H, Sun JM, Pazin MJ, Davie JR, Peterson CL (2006) Histone H4-K16 acetylation controls chromatin structure and protein interactions. *Science* **311:** 844-847

Siebel AL, Fernandez AZ, El-Osta A (2010) Glycemic memory associated epigenetic changes. *Biochemical pharmacology* **80:** 1853-1859

Smith BC, Denu JM (2009) Chemical mechanisms of histone lysine and arginine modifications. *Biochimica et biophysica acta* **1789:** 45-57

Smyth S, Heron A (2006) Diabetes and obesity: the twin epidemics. *Nature medicine* **12:** 75-80

Stassi G, Garofalo M, Zerilli M, Ricci-Vitiani L, Zanca C, Todaro M, Aragona F, Limite G, Petrella G, Condorelli G (2005) PED mediates AKT-dependent chemoresistance in human breast cancer cells. *Cancer research* **65:** 6668-6675

Struhl K (1998) Histone acetylation and transcriptional regulatory mechanisms. *Genes & development* **12:** 599-606

Tateishi K, Okada Y, Kallin EM, Zhang Y (2009) Role of Jhdm2a in regulating metabolic gene expression and obesity resistance. *Nature* **458:** 757-761

Taylor R (2008) Pathogenesis of type 2 diabetes: tracing the reverse route from cure to cause. *Diabetologia* **51:** 1781-1789

Teperino R, Schoonjans K, Auwerx J (2010) Histone methyl transferases and demethylases; can they link metabolism and transcription? *Cell metabolism* **12:** 321-327

Trencia A, Fiory F, Maitan MA, Vito P, Barbagallo AP, Perfetti A, Miele C, Ungaro P, Oriente F, Cilenti L, Zervos AS, Formisano P, Beguinot F (2004) Omi/HtrA2 promotes cell death by binding and degrading the anti-apoptotic protein ped/pea-15. *The Journal of biological chemistry* **279:** 46566-46572

Tsukada Y, Fang J, Erdjument-Bromage H, Warren ME, Borchers CH, Tempst P, Zhang Y (2006) Histone demethylation by a family of JmjC domain-containing proteins. *Nature* **439:** 811-816

Ungaro P, Mirra P, Oriente F, Nigro C, Ciccarelli M, Vastolo V, Longo M, Perruolo G, Spinelli R, Formisano P, Miele C, Beguinot F (2012) Peroxisome proliferator-activated receptor-gamma activation enhances insulin-stimulated glucose disposal by reducing ped/pea-15 gene expression in skeletal muscle cells: evidence for involvement of activator protein-1. *The Journal of biological chemistry* **287:** 42951-42961

Ungaro P, Teperino R, Mirra P, Cassese A, Fiory F, Perruolo G, Miele C, Laakso M, Formisano P, Beguinot F (2008) Molecular cloning and characterization of the human PED/PEA-15 gene promoter reveal antagonistic regulation by hepatocyte nuclear factor 4alpha and chicken ovalbumin upstream promoter transcription factor II. *The Journal of biological chemistry* **283:** 30970-30979

Ungaro P, Teperino R, Mirra P, Longo M, Ciccarelli M, Raciti GA, Nigro C, Miele C, Formisano P, Beguinot F (2010) Hepatocyte nuclear factor (HNF)-4alpha-driven epigenetic silencing of the human PED gene. *Diabetologia* **53:** 1482-1492

Valentino R, Lupoli GA, Raciti GA, Oriente F, Farinaro E, Della Valle E, Salomone M, Riccardi G, Vaccaro O, Donnarumma G, Sesti G, Hribal ML, Cardellini M, Miele C, Formisano P, Beguinot F (2006) The PEA15 gene is overexpressed and related to insulin resistance in healthy first-degree relatives of patients with type 2 diabetes. *Diabetologia* **49:** 3058-3066

Vigliotta G, Miele C, Santopietro S, Portella G, Perfetti A, Maitan MA, Cassese A, Oriente F, Trencia A, Fiory F, Romano C, Tiveron C, Tatangelo L, Troncone G, Formisano P, Beguinot F (2004) Overexpression of the ped/pea-15 gene causes diabetes by impairing glucose-stimulated insulin secretion in addition to insulin action. *Molecular and cellular biology* **24:** 5005-5015

Visel A, Rubin EM, Pennacchio LA (2009) Genomic views of distant-acting enhancers. *Nature* **461:** 199-205

Wellen KE, Hatzivassiliou G, Sachdeva UM, Bui TV, Cross JR, Thompson CB (2009) ATP-citrate lyase links cellular metabolism to histone acetylation. *Science* **324:** 1076-1080

Weyer C, Bogardus C, Mott DM, Pratley RE (1999) The natural history of insulin secretory dysfunction and insulin resistance in the pathogenesis of type 2 diabetes mellitus. *The Journal of clinical investigation* **104:** 787-794

Wheatley KE, Nogueira LM, Perkins SN, Hursting SD (2011) Differential effects of calorie restriction and exercise on the adipose transcriptome in diet-induced obese mice. *Journal of obesity* **2011:** 265417

Xanthopoulos KG, Prezioso VR, Chen WS, Sladek FM, Cortese R, Darnell JE, Jr. (1991) The different tissue transcription patterns of genes for HNF-1, C/EBP, HNF-3, and HNF-4, protein factors that govern liver-specific transcription. *Proceedings of the National Academy of Sciences of the United States of America* **88:** 3807-3811

Xiao C, Yang BF, Asadi N, Beguinot F, Hao C (2002) Tumor necrosis factor-related apoptosis-inducing ligand-induced death-inducing signaling complex and its modulation by c-FLIP and PED/PEA-15 in glioma cells. *The Journal of biological chemistry* **277:** 25020-25025

Young NL, Dimaggio PA, Garcia BA (2010) The significance, development and progress of high-throughput combinatorial histone code analysis. *Cellular and molecular life sciences : CMLS* **67:** 3983-4000

Yuan JS, Reed A, Chen F, Stewart CN, Jr. (2006) Statistical analysis of real-time PCR data. *BMC bioinformatics* **7:** 85

Zaidi SK, Young DW, Montecino M, van Wijnen AJ, Stein JL, Lian JB, Stein GS (2011) Bookmarking the genome: maintenance of epigenetic information. *The Journal of biological chemistry* **286:** 18355-18361

Zeggini E (2007) A new era for Type 2 diabetes genetics. *Diabetic medicine : a journal of the British Diabetic Association* **24:** 1181-1186

Zhang Y, Redina O, Altshuller YM, Yamazaki M, Ramos J, Chneiweiss H, Kanaho Y, Frohman MA (2000) Regulation of expression of phospholipase D1 and D2 by PEA-15, a novel protein that interacts with them. *The Journal of biological chemistry* **275:** 35224-35232

Gene Regulation:

Peroxisome Proliferator-activated Receptor- γ Activation Enhances Insulin-stimulated Glucose Disposal by Reducing *ped/pea-15* Gene Expression in Skeletal Muscle Cells: EVIDENCE FOR INVOLVEMENT OF ACTIVATOR PROTEIN-1

Paola Ungaro, Paola Mirra, Francesco Oriente, Cecilia Nigro, Marco Ciccarelli, Viviana Vastolo, Michele Longo, Giuseppe Perruolo, Rosa Spinelli, Pietro Formisano, Claudia Miele and Francesco Beguinot

J. Biol. Chem. 2012, 287:42951-42961.
doi: 10.1074/jbc.M112.406637 originally published online October 26, 2012

THE JOURNAL OF BIOLOGICAL CHEMISTRY VOL. 287, NO. 51, pp. 42951–42961, December 14, 2012

Peroxisome Proliferator-activated Receptor-γ Activation Enhances Insulin-stimulated Glucose Disposal by Reducing *ped/pea-15* Gene Expression in Skeletal Muscle Cells

EVIDENCE FOR INVOLVEMENT OF ACTIVATOR PROTEIN-1[*]

Received for publication, July 31, 2012, and in revised form, October, 25, 2012 Published, JBC Papers in Press, October 26, 2012, DOI 10.1074/jbc.M112.406637

Paola Ungaro[‡1,2], **Paola Mirra**[‡1], **Francesco Oriente**[§], **Cecilia Nigro**[‡], **Marco Ciccarelli**[§], **Viviana Vastolo**[‡§], **Michele Longo**[‡], **Giuseppe Perruolo**[‡], **Rosa Spinelli**[§], **Pietro Formisano**[§], **Claudia Miele**[‡], **and Francesco Beguinot**[‡§]

From the [§]*Dipartimento di Biologia e Patologia Cellulare e Molecolare, Università di Napoli "Federico II" and the* [‡]*Istituto di Endocrinologia e Oncologia Sperimentale Gaetano Salvatore, Consiglio Nazionale delle Ricerche, 80131 Naples, Italy*

Background: PPARγ modulation of glucoregulatory response in skeletal muscle has been only partially elucidated.
Results: PPARγ inhibits the transcription of the diabetes-associated gene *ped/pea-15* via AP-1.
Conclusion: *ped/pea-15* is downstream of a PPARγ-regulated inflammatory network.
Significance: These studies further elucidate the gene network responsible for inflammation-induced insulin resistance.

The gene network responsible for inflammation-induced insulin resistance remains enigmatic. In this study, we show that, in L6 cells, rosiglitazone- as well as pioglitazone-dependent activation of peroxisome proliferator-activated receptor-γ (PPARγ) represses transcription of the *ped/pea-15* gene, whose increased activity impairs glucose tolerance in mice and humans. Rosiglitazone enhanced insulin-induced glucose uptake in L6 cells expressing the endogenous *ped/pea-15* gene but not in cells expressing *ped/pea-15* under the control of an exogenous promoter. The ability of PPARγ to affect *ped/pea-15* expression was also lost in cells and in C57BL/6J transgenic mice expressing *ped/pea-15* under the control of an exogenous promoter, suggesting that *ped/pea-15* repression may contribute to rosiglitazone action on glucose disposal. Indeed, high fat diet mice showed insulin resistance and increased *ped/pea-15* levels, although these effects were reduced by rosiglitazone treatment. Both supershift and ChIP assays revealed the presence of the AP-1 component c-JUN at the *PED/PEA-15* promoter upon 12-*O*-tetradecanoylphorbol-13-acetate stimulation of the cells. In these experiments, rosiglitazone treatment reduced c-JUN presence at the *PED/PEA-15* promoter. This effect was not associated with a decrease in c-JUN expression. In addition, c-*jun* silencing in L6 cells lowered *ped/pea-15* expression and caused nonresponsiveness to rosiglitazone, although c-*jun* overexpression enhanced the binding to the *ped/pea-15* promoter and blocked the rosiglitazone effect. These results indicate that PPARγ regulates *ped/pea-15* transcription by inhibiting c-JUN binding at the *ped/pea-15* promoter. Thus, *ped/pea-15* is downstream of a major PPARγ-regulated inflammatory network. Repression of *ped/pea-15* transcription might contribute to the PPARγ regulation of muscle sensitivity to insulin.

Peroxisome proliferator-activated receptor-γ (PPARγ)[3] is a member of the nuclear hormone receptor superfamily. In addition to other PPAR isoforms, this superfamily also includes the receptors for thyroid hormones, retinoids, steroid hormones, and vitamin D (1, 2). PPARγ regulates gene transcription by binding with the retinoid X receptors to specific DNA sequences termed peroxisome proliferator response elements (3). After ligand activation, PPARγ modifies its conformation, which facilitates the release of corepressors and subsequent binding of a distinct set of nuclear coactivators, thereby fostering PPARγ action (3). Ultimately, formation of these transcriptional complexes enables PPARγ transcriptional control of a variety of biological processes, including insulin sensitivity (4). Indeed, PPARγ exerts important modulatory actions upstream of the major inflammatory networks involving AP-1 and NF-κB transcriptional regulation (5).

PPARγ activation by thiazolidinediones (TZDs) markedly improves insulin sensitivity in type 2 diabetic patients (6–9). However, the molecular mechanisms responsible for PPARγ-mediated insulin sensitization have been only partially defined. Studies in tissue-specific PPARγ knock-out mice have generated insight into the role of different tissues in PPARγ-mediated regulation of systemic insulin-stimulated glucose metabolism (10) (2, 11). To date, the relevance of PPARγ in maintaining systemic insulin sensitivity in adipose tissues has been convincingly demonstrated. In fact, the PPARγ-mediated adipogenesis associated with the capability for fatty acid trapping has emerged as a major factor in protecting against non-adipose tissue insulin resistance (12). Skeletal muscle expression of PPARγ has further been shown to contribute to systemic insulin sensitivity by maintaining intact insulin-mediated glucose utilization in muscle (10). Indeed, PPARγ was reported to directly coordinate glucoregulatory responses in this tissue (11). However, the genetic network responsible for

* This study was supported in part by European Community FP6 PREPOBEDIA Grant 201681, the European Foundation for the Study of Diabetes, the Associazione Italiana per la Ricerca sul Cancro, and by Ministero dell'Università e della Ricerca Scientifica Grants PRIN and FIRB-MERIT.
[1] Both authors contributed equally to this work.
[2] To whom correspondence should be addressed. E-mail: pungaro@ieos.cnr.it.

[3] The abbreviations used are: PPARγ, peroxisome proliferator-activated receptor-γ; TZD, thiazolidinedione; Ptz, pioglitazone; TPA, 12-*O*-tetradecanoylphorbol-13-acetate; qRT-PCR, quantitative RT-PCR; Rtz, rosiglitazone; CRE, cAMP-response element.

these functions in skeletal muscle has not been completely elucidated yet.

Phosphoprotein Enriched in Diabetes/Phosphoprotein Enriched in Astrocytes (PED/PEA-15) is a scaffold cytosolic protein widely expressed in most human tissues (13, 14). Early studies indicated that PED/PEA-15 has an important role in controlling glucose disposal in the skeletal muscle by impacting on the phospholipase D/protein kinase C signaling network (15, 16). Further investigations demonstrated that PED/PEA-15 is commonly overproduced in individuals with type 2 diabetes as well as in their euglycemic offspring, causing skeletal muscle insulin resistance in these individuals (17). PED/PEA-15 cellular levels are regulated by ubiquitinylation and proteosomal degradation (18). In addition, run-on experiments in cultured cells from type 2 diabetic patients have demonstrated that PED/PEA-15 overproduction is caused, at least in part, by transcriptional abnormalities (13). More recent studies evidenced that epigenetic changes at the *PED/PEA-15* gene have a major role in controlling its transcription (19). However, the molecular details responsible for regulation of *PED/PEA-15* transcription as well as the abnormalities in these mechanisms occurring in type 2 diabetes remain unclear.

In this report, we demonstrate that PPARγ represses the transcription of the diabetes-associated gene *ped/pea-15*. We found that PPARγ repression of this gene requires displacement of the c-JUN component of the AP-1 transcriptional complex from the *ped/pea-15* promoter. These findings identify *ped/pea-15* as a gene downstream of major PPARγ-regulated inflammatory networks, whose control may be instrumental to PPARγ action on glucose disposal by the skeletal muscle.

EXPERIMENTAL PROCEDURES

Materials—Rosiglitazone and pioglitazone (Ptz) were purchased from Cayman Chemical (Ann Arbor, MI). 12-*O*-Tetradecanoylphorbol-13-acetate (TPA) and GW9662 were purchased from Sigma. Solutions were prepared in dimethyl sulfoxide (DMSO) and diluted 1:1000 into serum-free DMEM immediately before use. PPARγ, c-JUN, and 14-3-3ϵ antibodies were purchased from Santa Cruz Biotechnology (Santa Cruz, CA), and the PED/PEA-15 antibody was purchased from Cell Signaling Technology (Danvers, MA). Oligonucleotides, including the scrambled phosphorothioate oligodeoxynucleotide and the rat c-Jun antisense (20), were synthesized by Sigma. [γ-^{32}P]dATP and 2-[1-^{14}C]deoxy-D-glucose, were purchased from PerkinElmer Life Sciences. The pPED2000-Luc and pPED210-Luc constructs have been previously described (21). Site-directed mutagenesis of the CRE-like site was achieved using the QuikChange site-directed mutagenesis kit according to the manufacturer's instructions (Stratagene, La Jolla, CA). The following oligonucleotides were validated by EMSA and used to create the desired mutation: CREmut.F 5′-CCGGCTCTGACATTGCCGGCCAGCCGGG-3′ and CREmut.R 5′-CCCGGCTGGCCGGCAATGTCAGAGCCGG-3′. Mutant clones were screened by DNA sequencing. The pcDNA3 expression vector containing the Myc-tagged PED/PEA-15 has also been reported previously (22). The (PPRE)3-tk-luciferase construct (23) was donated by Dr. Mitchell Lazar (University of Pennsylvania). The dominant negative PPARγ expression vector, the L468A/E471A h-PPARγ double mutant (24), was donated by V. Krishna K. Chatterjee from University of Cambridge, United Kingdom. The expression vector (pCEFL) for c-Jun-HA was provided by Dr. Musti (University of Cosenza, Italy).

Cell Culture Studies—L6 skeletal muscle cells and HeLa cells were cultured in Dulbecco's modified Eagle's medium (DMEM) supplemented with 10% fetal bovine serum (FBS) and 1% penicillin/streptomycin solution at 37 °C in a humidified 95% air and 5% CO_2 atmosphere. L6 myoblasts were plated at a density of 3×10^4 cells/ml, and differentiation of confluent cells was initiated by reducing the FBS content of the media to 2% with a medium change every 48 h. Differentiation of myoblasts into multinucleated myotubes was completed by 7 days after medium change. Fused multinucleated myotubes were incubated with the serum-depleted (0.5%) medium for 16 h and treated with TZDs at the indicated concentrations for a further 24 h, although control cells received the vehicle alone in the serum-depleted (0.5%) medium. L6 myoblasts were electroporated with the Neon Transfection System (Invitrogen), and L6 myotubes and HeLa cells were transfected using Lipofectamine 2000 (Invitrogen), according to the manufacturer's instructions (15). All cell culture media and reagents were from Lonza (Basel, Switzerland).

Glucose uptake in L6 cells was assayed as reported previously (25). Briefly, the cells were incubated for 24 h in serum-free medium supplemented with 0.25% (w/v) bovine serum albumin (BSA) in the absence or presence of 1 μM Rtz. The cells were rinsed in glucose-free HEPES buffer (5 mM KCl, 120 mM NaCl, 1.2 mM $MgSO_4$, 10 mM $NaHCO_3$, 1.2 mM $KHPO_4$, and 20 mM HEPES, pH 7.8, 2% albumin) and further exposed to 100 nM insulin for 30 min. 2-Deoxy-D-[^{14}C]glucose uptake was measured over a 10-min period, with nonspecific uptake determined in the presence of cytochalasin-B.

Animal Studies—5-Week-old male C57BL/6J mice were hosted at the common facility of the University of Naples Medical School and had free access to water and food. For high fat diet treatment, mice were fed a high fat diet with ~60 cal % fat or a standard diet with ~10 cal % fat (Research Diets, New Brunswick, NJ) (26) for 12 weeks. During the last 10 days, the animals received either 10 mg/kg/die Rtz or vehicle alone (0.5% carboxymethylcellulose) by oral gavage. For insulin tolerance testing, mice were fasted for 4 h and then subjected to intraperitoneal injection with insulin (0.75 milliunits g^{-1} of body weight). Venous blood was subsequently drawn by tail clipping at 0, 15, 30, 45, 60, 90, and 120 min as in Ref. 27. For intraperitoneal glucose tolerance testing, mice were fasted overnight and then subjected to intraperitoneal injection with glucose (2.0 g kg^{-1} of body weight). Venous blood was subsequently drawn by tail clipping at 0, 15, 30, 45, 60, 90, and 120 min as in Ref. 27. In overnight fasted mice, serum insulin concentrations were measured by rat insulin RIA kit (Millipore, Billerica, MA) (27). Blood glucose levels were measured with Accu-Chek® glucometers (Roche Applied Science). In overnight fasted mice, analyses of serum triglycerides, total cholesterol, HDL cholesterol, and LDL cholesterol were done on Horiba ABX Pentra 400 Chemistry Analyzer (HORIBA ABX, Montpellier, France). The animals were sacrificed, and skeletal muscle tissues (gas-

trocnemius) were removed, rinsed with 0.9% NaCl, frozen in liquid nitrogen, and kept in −80 °C before harvesting.

Western Blot Analysis—Cells were solubilized by scraping and passed 10 times through a 25-gauge needle in ice-cold lysis buffer, supplemented with the Complete Protease Inhibitor Mixture Tablets (Roche Applied Science). Lysates were clarified by centrifugation at 16,000 × *g* for 10 min at 4 °C, and protein concentration was determined using the protein assay based on Bradford's method (Bio-Rad) (28). Total cell extracts in equal amounts were separated by SDS-PAGE and blotted on nitrocellulose membranes (Millipore, Billerica, MA). Membranes were blocked in 5% BSA, and specific proteins were detected by incubation with appropriate primary and secondary antibodies (horseradish peroxidase-conjugated) in 150 mM NaCl, 50 mM Tris, 0.5% Tween 20 (TBST). Protein bands were visualized using an enhanced chemiluminescence (ECL) kit (Thermo Scientific Pierce Protein Biology, Waltham, MA) and quantified by the ImageJ software (a public domain and Java-based image processing program developed at the National Institutes of Health). Relative protein abundance was calculated after 14-3-3ϵ normalization.

Real Time PCR Analysis—Total RNA was extracted with the TRIzol reagent (Invitrogen), according to the manufacturer's protocol. Reverse transcription of 1 μg of total RNA was performed using SuperScript III (Invitrogen), following the manufacturer's instructions. Quantitative real time PCR was performed in triplicate by using iQ SYBR Green Supermix on iCycler real time detection system (Bio-Rad). Relative quantification of gene expression was calculated by the ΔΔ*Ct* method (29). Each *Ct* value was first normalized to the respective glyceraldehyde-3-phosphate dehydrogenase (GAPDH) *Ct* value of a sample to account for variability in the concentration of RNA and in the conversion efficiency of the RT reaction. For copy number analysis, the real time PCR amplification products for *ped/pea-15* and *gapdh* were cloned into the pGEM®-T easy vector (Promega, Madison, WI), and calibration curves were made from serial 10-fold dilutions of plasmid DNAs as described previously (30). The mean slopes of the calibration curves for the two genes were similar, −3.3 for *ped/pea-15* and −3.1 for *gapdh*, where a slope of −3.3 ± 10% reflects an efficiency of 100 ± 10% of the PCR r, and the mean correlation coefficient (*R*) for both of the curves was 0.99. The equations drawn from the graph of the standard curves were used to calculate the precise number of specific cDNA molecules present in the samples (copy number variation).

Luciferase Assays—Cells were cotransfected with 2 μg of the Firefly luciferase vector (pGL3 plasmids, Promega, Madison, WI) and 1 μg of the pRSV-β-galactosidase (Promega, Madison, WI), as internal control to normalize for transfection efficiency. In each reaction, the total amount of transfected DNA was kept constant at 5 μg by using the empty expression vector pcDNA3 or PPARγ$_{L468A/E471A}$ mutant. 24 h after transfection, cells were incubated with the serum-depleted (0.5%) medium for 16 h and then exposed to serum-depleted (0.5%) medium supplemented with vehicle (0.1% DMSO) or TPA (0.1 μM) in the absence or presence of increasing concentrations of Rtz for 4 h. Luciferase and β-galactosidase activities were measured with a luminometer (Berthold Technologies, Bad Wildbad, Germany). Luciferase activities were divided by the respective β-galactosidase activity and expressed as relative luciferase units.

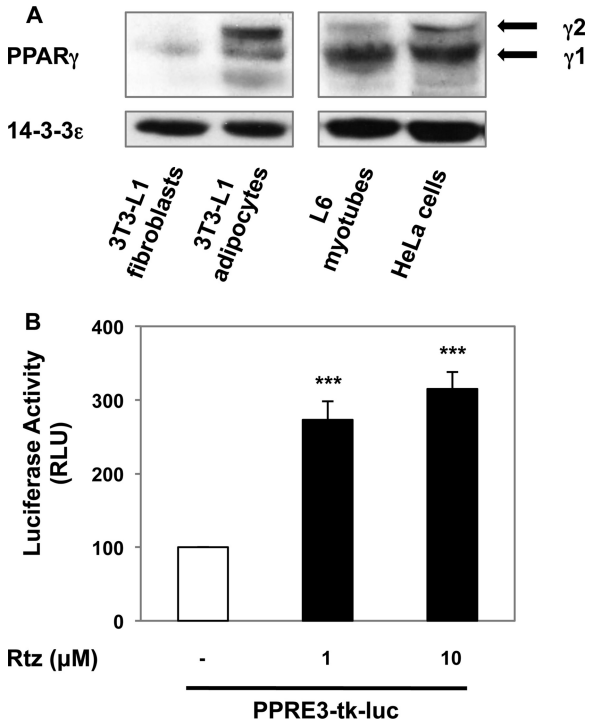

FIGURE 1. **PPARγ expression and function in L6 skeletal muscle cells.** *A*, 3T3-L1 fibroblasts, 3T3-L1 adipocytes, L6 myotubes, and HeLa cells were lysed, and total protein extracts were separated by SDS-PAGE. The antibodies used were specific for PPARγ and 14-3-3ϵ as loading control. The autoradiograph shown is representative of four additional experiments. *B*, L6 myotubes were cotransfected with PPRE3-tk-luc and pRSV-β-gal constructs as described under "Experimental Procedures." Upon transfection, the cells were incubated in the absence or presence of the indicated concentrations of Rtz. Luciferase and β-galactosidase activities were measured in cellular extracts 24 h later. β-Galactosidase activity enabled the estimation of transfection efficiency and assessment of relative luciferase values (*RLU*). *Bars* represent the means ± S.D. of three independent experiments. *Asterisks* indicate statistically significant differences at a $p < 0.001$ level.

Electrophoretic Mobility Gel Shift (EMSA) and Supershift Assays—Nuclear extracts from HeLa cells were prepared as described previously with minor modifications (31). Double-stranded oligonucleotides were end-labeled with [γ-^{32}P]ATP by T4 polynucleotide kinase (Promega, Madison, WI) according to the manufacturer's instructions. The radiolabeled probes were purified by spin columns (Roche Applied Science). 5 μg of nuclear protein extracts from control and treated cells were incubated with 100,000 cpm ^{32}P-labeled oligonucleotide probe in 25 mM HEPES, pH 7.4, 50 mM KCl, 10% glycerol (v/v), 5 mM dithiothreitol (DTT), and 1 μg of poly(dI-dC) (GE Healthcare) for 30 min at room temperature in a final volume of 20 μl. Upon binding, protein-DNA complexes were separated on 6% non-denaturing polyacrylamide gels at 120 V in 0.5× TBE buffer. Gels were dried and further subjected to PhosphorImager analysis (Bio-Rad). In competition analysis, 25-, 50-, and 100-fold molar excess of the unlabeled double strand oligonucleotide was added to the reaction mixture prior to the addition of the labeled probe. For the antibody supershift analysis, 1 μg of antibody was added to the nuclear extracts prior to the radiolabeled oligonucleotide.

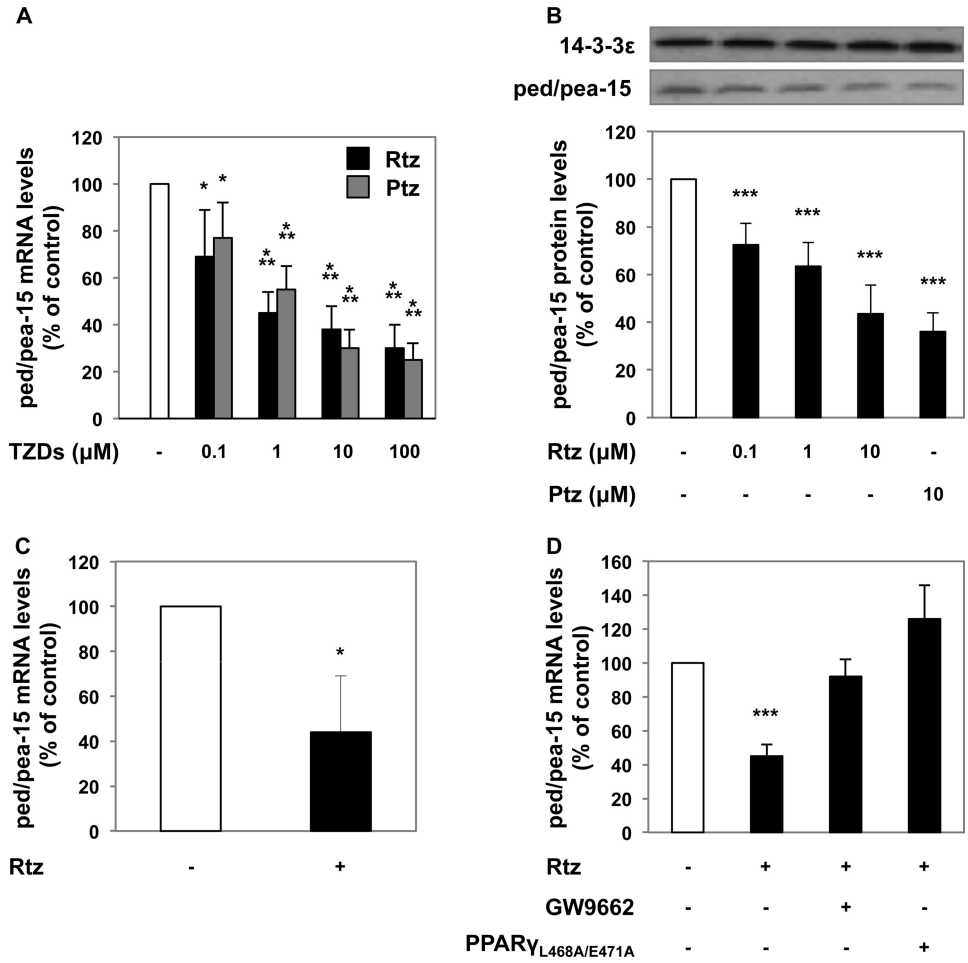

FIGURE 2. **PPARγ repression of *ped/pea-15* transcription.** *A,* L6 myotubes were incubated in the presence of the indicated concentrations of Rtz (*black bars*) or Ptz (*gray bars*) for 24 h. Total RNA was obtained, and *ped/pea-15* and *gapdh* mRNA levels were measured by qRT-PCR. Values were normalized for *gapdh* and presented as fold decrease relative to the control (untransfected cells). *B,* L6 myotubes were incubated in the absence or presence of Rtz for 24 h. Total protein extracts were separated by SDS-PAGE followed by immunoblotting with PED/PEA-15 or 14-3-3ϵ antibody, as indicated. The one presented is representative of two additional experiments with very similar results. *C,* total RNA was obtained from gastrocnemius of C57BL/6J mice treated or not with 10 mg/kg/die Rtz for 10 days. The mRNAs were assessed by qRT-PCR. *ped/pea-15* values were normalized for *gapdh* and expressed as fold decrease *versus* control. *D,* L6 myotubes were preincubated with 10 μM GW9662 for 1 h or transfected with the $PPAR\gamma_{L468A/E471A}$ mutant as described under "Experimental Procedures" and then treated with 1 μM Rtz for 24 h. Total RNA was obtained, and *ped/pea-15* and *gapdh* mRNA levels were measured by qRT-PCR. Values were normalized for *gapdh* and presented as fold decrease relative to the control. *Bars* represent the means ± S.D. of three (*A* and *D*) and four independent experiments (*B*). Five mice/group were used in *C*. *Asterisks* denote statistically significant differences (*, $p < 0.05$; **, $p < 0.01$, and ***, $p < 0.001$).

Chromatin Immunoprecipitation Assay (ChIP)—ChIP assays were performed as reported previously (21). Briefly, upon protein-DNA cross-linking, cells were lysed and sonicated to achieve chromatin fragments ranging between 500 and 1000 bp in size. The lysates were incubated with either c-JUN antibody or a rabbit control IgG, and then complexes were isolated using protein A-agarose/salmon sperm DNA (Millipore, Billerica, MA). Immunoprecipitates were extensively washed and then eluted by freshly prepared 1% SDS, 0.1 M $NaHCO_3$ buffer. After reversion of cross-linking, DNA was purified by the QIAquick PCR purification kit (Qiagen, Hilden, Germany) followed by PCR amplification. PCR products were resolved by 2% agarose gel electrophoresis, revealed by ethidium bromide staining, and analyzed by densitometry using the ImageJ software (National Institutes of Health).

Statistical Analysis—All data are presented as means ± S.E. Statistical differences were determined by one- or two-way analysis of variance as appropriate, and Bonferroni post hoc testing was performed when applicable. A p value <0.05 was considered significant.

RESULTS

PPARγ Regulates ped/pea-15 Function in Muscle Cells—We assessed PPARγ expression in the L6 skeletal muscle cell line by Western blot analysis. The PPAR-specific antibody detected both the isoforms 1 and 2, which have a predicted molecular mass of ~53 and 57 kDa, respectively. In L6 myotubes as well as in HeLa cells, the γ1 isoform was more abundant than the γ2 isoform, although PPARγ2 was the most highly expressed isoform in 3T3-L1 adipocytes. At variance, 3T3-L1 fibroblasts showed very low PPARγ levels (Fig. 1*A*). L6 cells were also transfected with a construct featuring the PPAR response element upstream from the luciferase gene (PPRE3-tk-luc). As shown in Fig. 1*B*, treatment of these cells with increasing amounts of the PPARγ agonist Rtz determined a significant

increase in the promoter activity, indicating that PPARγ is transcriptionally active in L6 cells.

PPARγ has been reported to regulate a number of genes controlling metabolic functions (32). Interestingly, in L6 myotubes, Rtz and Ptz repressed *ped/pea-15* expression in a dose-dependent manner, and this effect occurred both at mRNA (Fig. 2*A*) and at protein levels (Fig. 2*B*). A comparable decrease in *ped/pea-15* mRNA levels was also observed in the skeletal muscle of Rtz-treated C57BL/6J mice (Fig. 2*C*). In addition, both pretreatment of L6 cells with the PPARγ antagonist GW9662 and transfection with the dominant negative PPARγ mutant, $PPAR\gamma_{L468A/E471A}$, completely abolished the Rtz effect (Fig. 2*D*), indicating that TZDs inhibit *ped/pea-15* expression via PPARγ.

The known physiological importance of PED/PEA-15 in regulating glucose tolerance prompted us to further investigate the molecular details of the TZDs action on ped/pea-15 function. To this end, we transfected L6 cells with a *myc*-tagged *PED/PEA-15* cDNA driving the expression of the gene under the control of the cytomegalovirus (CMV) promoter, and then we exposed the cells to Rtz. As shown in Fig. 3*A*, Rtz did not affect the levels of the exogenous PED/PEA-15 protein (21 kDa), although it reduced the levels of the endogenous one (15 kDa). Consistent with these findings, treatment with Rtz did not significantly affect PED/PEA-15 protein levels in the skeletal muscle of transgenic mice overexpressing this gene under the control of the exogenous β-actin promoter (Tg_{ped}), although it reduced endogenous PED/PEA-15 protein levels up to 60% in their wild-type littermates (Fig. 3*B*). Furthermore, as shown in Fig. 3*C*, Rtz enhanced glucose uptake in wild-type L6 cells ($L6_{WT}$) but not in those cells expressing the exogenous PED/PEA-15 ($L6_{ped}$). Thus, it appeared that the endogenous *ped/pea-15* promoter is necessary for PPARγ regulation of the gene.

PPARγ Silences ped/pea-15 by Interfering with AP-1 Signaling—These findings led us to explore the molecular mechanisms involved in PPARγ regulation of *ped/pea-15* in greater detail and to identify the PPARγ responding region at the *ped/pea-15* promoter. Previous studies in cells treated with TPA, a known activator of both AP-1 and NF-κB, revealed increased *PED/PEA-15* expression (18). We have therefore addressed the hypothesis that PPARγ reduces *PED/PEA-15* transcription by transrepressing one or both of these transcription factors. *In silico* analysis of the human *PED/PEA-15* promoter revealed the presence of a TGACATCA CRE-like site between the positions −106 and −86 bp from the transcription start site (+1). This sequence is known to bind the AP-1 transcriptional complex (33). A caGGGActtt NF-κB-binding site between positions −798 and −786 bp was also identified. Furthermore, sequence alignment of the human and rat 5′-flanking regions revealed that these two sequences are highly conserved, suggesting they may perform a major role in regulating *PED/PEA-15* expression and prompted us to test the significance of AP-1 and NF-κB in the PPARγ-dependent regulation of the *PED/PEA-15* promoter.

To this goal, we transfected HeLa cells with a reporter vector featuring the *luciferase* gene downstream from the −1942 to +58 bp of the proximal 5′-flanking region of the human *PED/PEA-15* gene (pPED2000). In these transfected cells, TPA up-

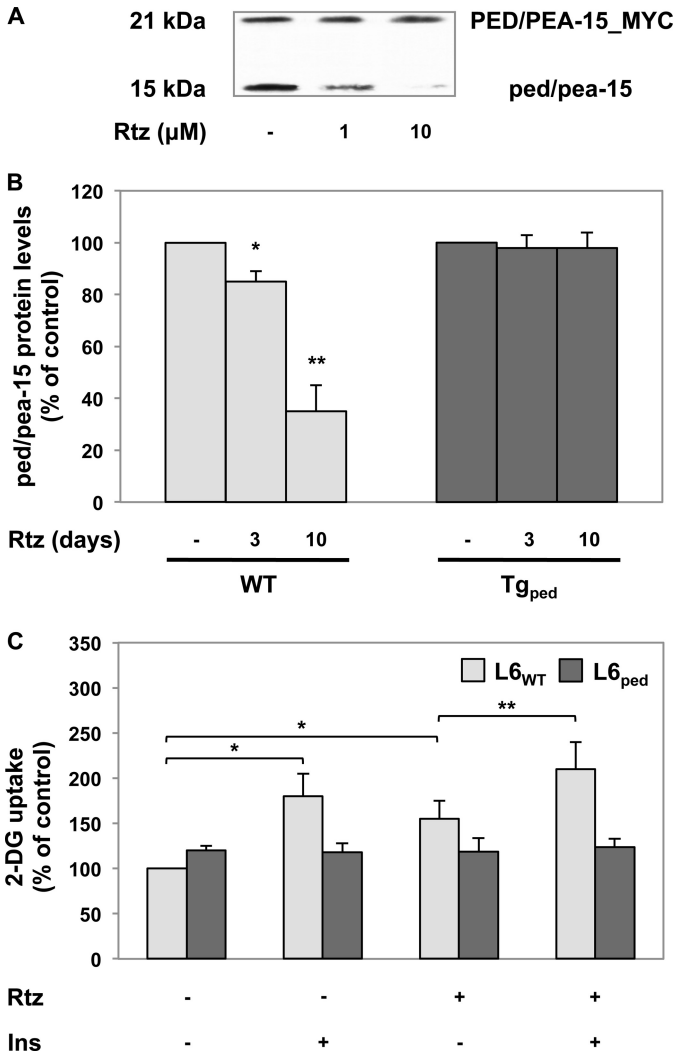

FIGURE 3. **Significance of *ped/pea-15* promoter to PPARγ-dependent repression.** *A*, L6 myotubes were transfected with a pcDNA3 expression vector containing a Myc-tagged *PED/PEA-15* cDNA under the control of the CMV promoter. The cells were incubated in the presence of the indicated concentrations of Rtz for 24 h. Total protein extracts were separated by SDS-PAGE and immunoblotted with a specific PED/PEA-15 antibody, which detected both the endogenous (15 kDa) and the exogenous (21 kDa) protein. Results are shown from a representative experiment; qualitatively similar data were obtained in replicate experiments. *B*, transgenic mice overexpressing PED/PEA-15 (Tg_{ped}; $n = 6$), and their nontransgenic littermates (WT; $n = 6$) were treated with 10 mg/kg/die of Rtz for either 3 or 10 days, as indicated. Total protein extracts from gastrocnemius were separated by SDS-PAGE followed by immunoblotting with PED/PEA-15 or 14-3-3ϵ antibody. Blots were revealed by ECL, and autoradiography and the intensity of bands was quantitated by densitometry. *C*, L6 myotubes were transfected with a *PED/PEA-15* cDNA (*dark gray bars*). Both $L6_{wt}$ and $L6_{ped}$ cells were incubated in the absence or presence of 1 μM Rtz for 24 h followed by stimulation with 100 nM insulin (*Ins*) for 30 min. 2-Deoxy-D-glucose (*2-DG*) uptake was assayed as described under "Experimental Procedures." *Bars* represent the means ± S.D. of duplicate (*B*) and triplicate (*C*) determinations in three independent experiments. *Asterisks* denote statistically significant differences (*, $p < 0.05$; **, $p < 0.01$).

regulated the *PED/PEA-15* promoter activity, achieving its maximum effect within 4 h of exposure (Fig. 4*A*). Consistently, a >2-fold increase in *PED/PEA-15* mRNA levels was also demonstrated by quantitative RT-PCR (qRT-PCR) analysis (Fig. 4*B*). Furthermore, TPA effect on both *PED/PEA-15* mRNA levels (Fig. 4*C*) and promoter activity (Fig. 4*D*) was significantly inhibited by treating the cells with Rtz. In addition, the presence

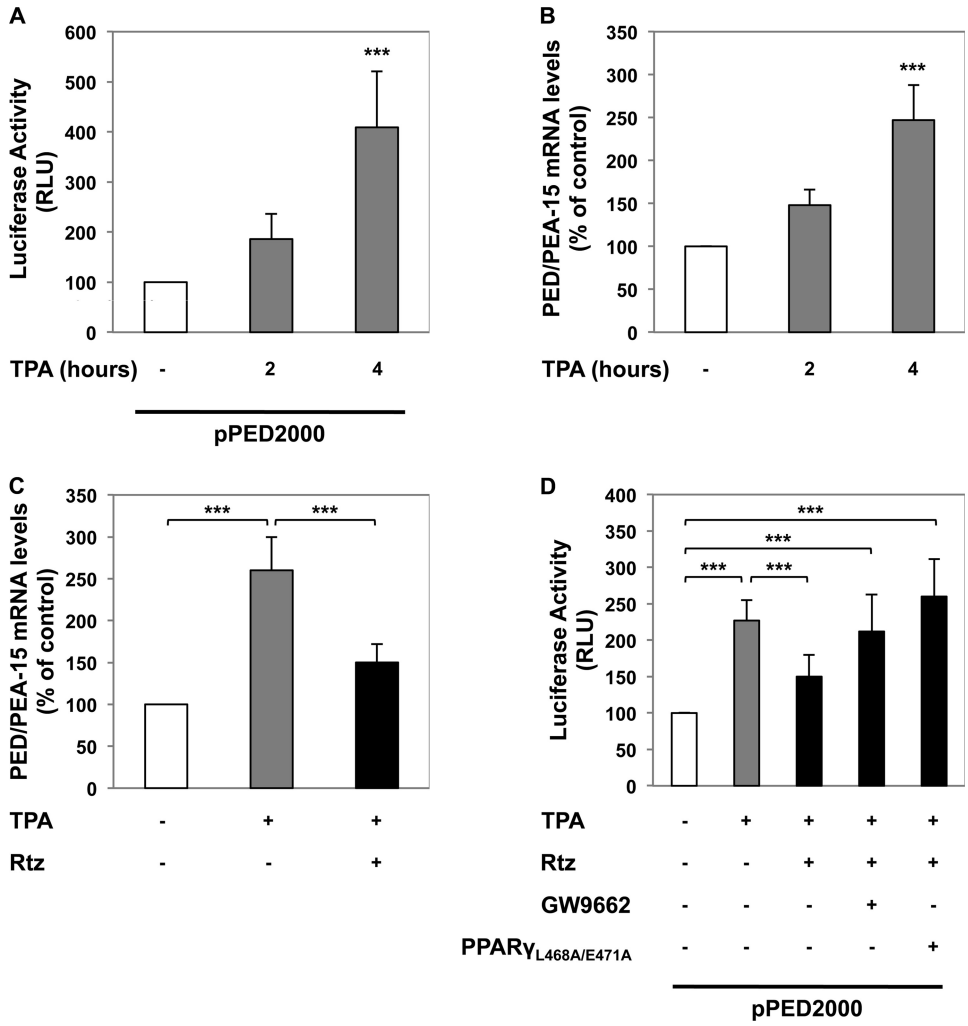

FIGURE 4. **Mechanisms of TPA regulation of *ped/pea-15* promoter activity.** *A* and *D*, HeLa cells, cotransfected with the pPED2000 and pRSV-β-gal constructs, were further transfected with the PPARγ$_{L468A/E471A}$ mutant or pretreated with 10 μM GW9662 for 1 h and subsequently incubated in the absence or presence of 0.1 μM TPA and 1 μM Rtz for 4 h, as indicated. Luciferase activities were measured and normalized for β-galactosidase activities. *Bars* represent the means ± S.D. of four independent experiments each performed in duplicate. *B* and *C*, HeLa cells were incubated in the absence or presence of 0.1 μM TPA and 1 μM Rtz for 4 h, as indicated. *PED/PEA-15* mRNA levels were subsequently quantitated by qRT-PCR, and values were normalized for *GAPDH* of the same samples and shown as fold increase relative to untreated cells. *Bars* represent the means ± S.D. of three independent experiments. *Asterisks* denote statistically significant differences (***, $p < 0.001$).

of the PPARγ antagonist GW9662 as well as that of the dominant negative PPARγ mutant, PPARγ$_{L468A/E471A}$, enabled full TPA effect on promoter activity during simultaneous treatment with Rtz (Fig. 4*D*). These findings initially supported the possibility that PPARγ regulation of *PED/PEA-15* function might involve AP-1 and/or NF-κB transcriptional control.

To further explore this hypothesis, we transfected HeLa cells with either a *PED/PEA-15* deletion construct lacking the NF-κB-binding site but featuring an intact CRE-like site (pPED210) or the same construct where the CRE-like site was mutagenized (pPED210$_{MUT}$). Interestingly, in the former case, exposure to TPA induced a 2.5-fold enhanced transcriptional activity, which was almost completely suppressed by Rtz treatment (Fig. 5*A*). At variance, cells transfected with the CRE-like mutagenized construct exhibited depressed basal promoter activity with complete loss of TPA responsiveness, whether in the absence or presence of Rtz. These observations led us to hypothesize that AP-1 plays a major role in basal and PPARγ-dependent regulation of *PED/PEA-15* expression. Indeed, in cells transfected with the pPED2000$_{MUT}$ construct, which features the intact NF-κB site but the mutated CRE-like site, Rtz treatment failed to repress TPA-induced *PED/PEA-15* promoter activity (Fig. 5*B*), suggesting that NF-κB is not involved in the regulation of *PED/PEA-15* expression by PPARγ.

EMSAs also revealed increased occupancy of the CRE-like site at *PED/PEA-15* promoter in lysates from TPA-treated as compared with untreated HeLa cells (Fig. 6*A*, *left*). This CRE-like site occupancy was dose-dependently inhibited by Rtz. Importantly, supershift assays with a specific c-JUN antibody revealed the presence of the AP-1 component c-JUN in the binding complex at the CRE-like site (Fig. 6*A*, *right*). c-JUN occupancy at the *PED/PEA-15* promoter was also investigated in living cells by ChIP assays. In these experiments, the cross-linked chromatin was precipitated using the c-JUN antibody followed by amplification of the CRE-like site at the human *PED/PEA-15* promoter. As shown in Fig. 6*B*, TPA exposure determined the c-JUN association to the CRE-like site, which was reduced by Rtz treatment in a dose-dependent manner.

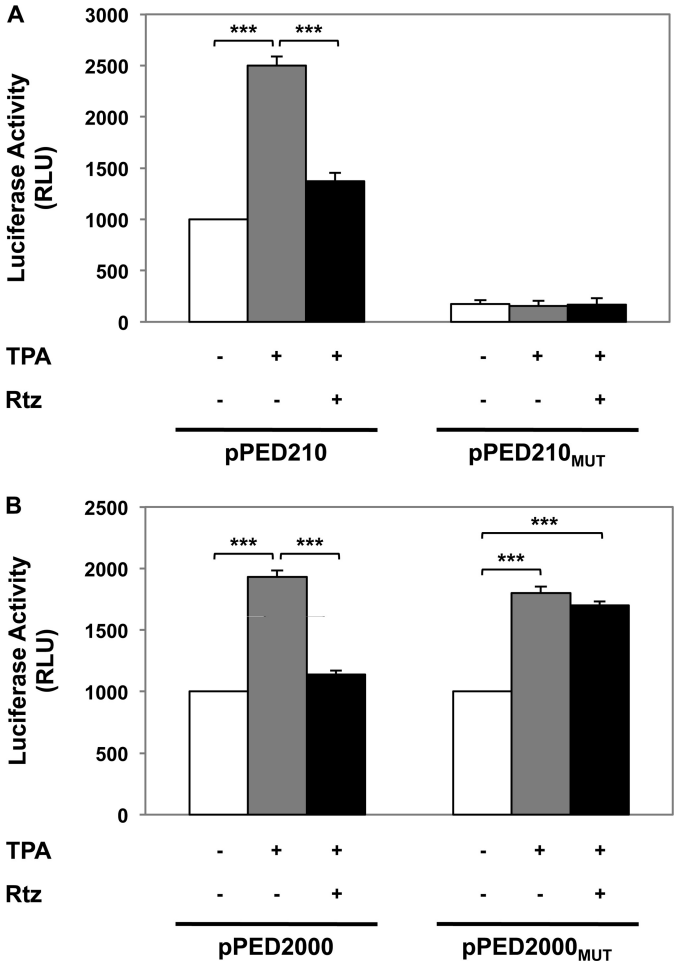

FIGURE 5. **Role of AP-1 in PPARγ-mediated regulation of *ped/pea-15* transcription.** HeLa cells were cotransfected with pPED210 (*A*) or pPED2000 (*B*) or the versions of these constructs featuring the mutagenized CRE-like site ($pPED210_{MUT}$ and $pPED2000_{MUT}$, respectively), in addition to pRSV-β-gal construct. The cells were then incubated in the absence or presence of 0.1 μM TPA and 1 μM Rtz for 4 h. Luciferase activities were normalized to β-galactosidase activities. Data are presented as means ± S.D. of four independent experiments, each in duplicate. *Asterisks* denote statistically significant differences (***, $p < 0.001$).

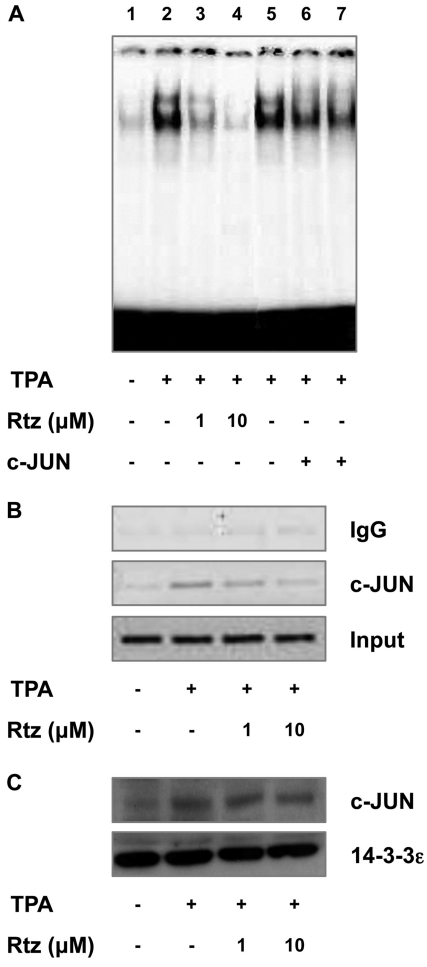

FIGURE 6. **Rtz effect on TPA-induced binding of AP-1 to the CRE-like site at *PED/PEA-15* promoter.** *A,* HeLa cells were incubated in the absence or presence of 0.1 μM TPA and the indicated concentrations of Rtz for 4 h (*lanes 1–4*). Nuclear protein extracts were incubated with a ^{32}P-labeled oligonucleotide encompassing the CRE-like site at *PED/PEA-15* promoter. Nuclear protein extracts from TPA-treated cells were preincubated with c-JUN antibody for different times (1 and 4 h, *lanes 6* and *7*) before adding the radiolabeled probe. The reaction mixtures were separated on 6% nondenaturing polyacrylamide gels, and dried gels were revealed by autoradiography. The autoradiographs shown are representative of four independent experiments. *B,* HeLa cells were incubated in the absence or presence of TPA and Rtz , as indicated; soluble chromatin was prepared and immunoprecipitated with either c-JUN or nonspecific IgG antibody. Chromatin immunoprecipitation was followed by PCR amplification with primers designed for the CRE-like site at the human *PED/PEA-15* promoter. Amplification products were separated on agarose gels and revealed by ethidium bromide. The photograph shown is representative of five independent experiments. *C,* cells were incubated in the absence or presence of TPA and Rtz, as indicated. Total protein extracts were separated by SDS-PAGE, transferred to nitrocellulose filters, and immunoblotted with c-JUN or 14-3-3ε antibody. Blots were revealed by ECL and autoradiography. The autoradiographs shown are representative of three independent experiments.

This effect was not due to a decrease in TPA-induced expression of c-JUN in HeLa cells (Fig. 6*C*).

PPARγ Represses ped/pea-15 Expression via AP-1 in L6 Cells—Based on ChIP assays, Rtz as well as Ptz treatment decreased c-jun binding to the CRE-like site also in L6 myotubes (Fig. 7*A*), confirming the major role of AP-1 in the *ped/pea-15* down-regulation by PPARγ also in skeletal muscle cells. Importantly, in these experiments, the two TZDs did not affect the binding of the NF-κB subunit p65 to its binding site on the *ped/pea-15* promoter (Fig. 7*B*).

In L6 cells, the overexpression of c-JUN (Fig. 8*A*) slightly increased *ped/pea-15* expression in untreated cells (Fig. 8*B*). However, higher levels of ectopic c-JUN bypassed the down-regulation of *ped/pea-15* due to PPARγ (Fig. 8*B*). In parallel, activated PPARγ was not able to displace c-JUN from the CRE-like site at *ped/pea-15* promoter when it was overexpressed in L6 cells (Fig. 8*C*). After c-jun silencing (Fig. 8*A*), L6 cells showed a significantly lower expression of *ped/pea-15* compared with wild-type cells no longer reduced by both Rtz and Ptz (Fig. 8*B*), supporting the major role of AP-1 in *ped/pea-15* down-regulation by PPARγ also in skeletal muscle cells.

PPARγ Decreases ped/pea-15 Expression in High Fat Diet-fed Mice—The *in vivo* significance of *ped/pea-15* regulation by PPARγ agonists was further explored in mice subjected to a high fat diet regimen for 12 weeks. As shown in Table 1, these mice became dyslipidemic and developed significant hyperinsulinemia and insulin resistance. Interestingly, these changes were accompanied by a 2.5-fold increase in *ped/pea-15* expression in their skeletal muscle. Further treatment of these mice

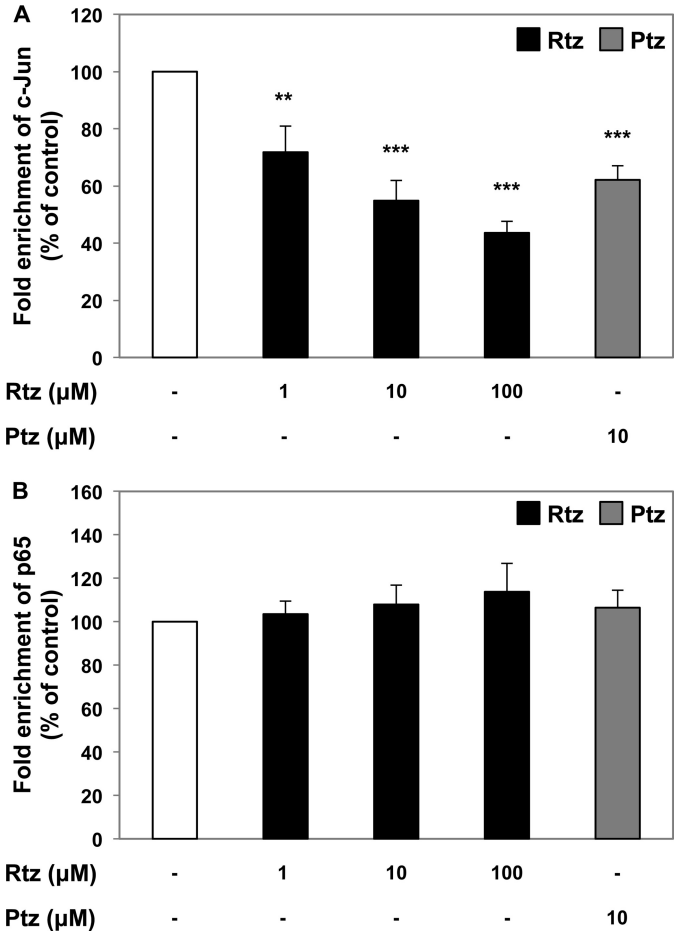

FIGURE 7. **TZD effect on *ped/pea-15* promoter occupancy by c-jun and p65.** L6 myotubes were incubated with either 10 μM Rtz or 10 μM Ptz for 24 h, as indicated. Soluble chromatin was prepared and immunoprecipitated with c-JUN, p65, or nonspecific IgG antibodies. Chromatin immunoprecipitation was followed by PCR amplification with primers designed for either the CRE-like site (*A*) or the NF-κB-binding site (*B*) at the rat *ped/pea-15* promoter. Amplification products were separated by agarose gels and revealed by ethidium bromide. *Bars* represent means ± S.D. of three independent experiments. *Asterisks* denote statistically significant differences (**, $p < 0.01$; ***, $p < 0.001$).

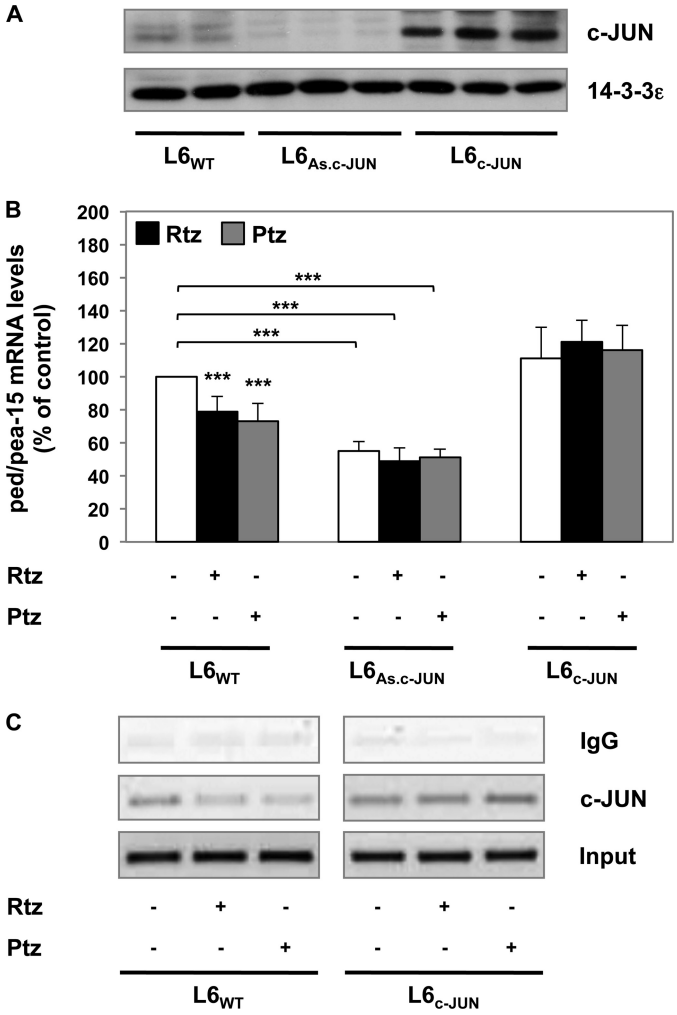

FIGURE 8. **Mechanism of TZD-dependent regulation of *ped/pea-15* expression.** L6 myotubes were transiently transfected with the vector pCEFL containing c-JUN cDNA or c-JUN phosphorothioate antisense oligonucleotides, as indicated. Upon transfection, the cells were incubated with either 10 μM Rtz or 10 μM Ptz for 24 h. *A,* cells were lysed, and total protein extracts were separated by SDS-PAGE followed by immunoblotting with c-JUN or 14-3-3ϵ antibody. Blots were revealed by ECL and autoradiography. *B,* total RNA was obtained, and then *ped/pea-15* and *gapdh* mRNA levels were measured by qRT-PCR. *Bars* represent the means ± S.D. of three independent experiments. *Asterisks* indicate statistically significant differences (*, $p < 0.05$; ***, $p < 0.001$). *C,* L6 myotubes were transiently transfected with the pCEFL containing a c-JUN cDNA before incubating with either 10 μM Rtz or 10 μM Ptz for 24 h. Soluble chromatin was prepared and immunoprecipitated with either c-JUN or nonspecific IgG antibody. Chromatin immunoprecipitation was followed by PCR amplification with primers designed for the CRE-like site at the rat *ped/pea-15* promoter. Amplification products were separated on agarose gels and revealed by ethidium bromide. The photograph shown is representative of three further experiments.

with Rtz for 10 days improved dyslipidemia and plasma insulin levels. Based on the determination of glucose areas under the curves during the accomplishment of insulin tolerance tests, insulin sensitivity was also rescued by Rtz. Simultaneously *ped/pea-15* mRNA levels were significantly reduced, further supporting the important role of *ped/pea-15* in Rtz action *in vivo*.

DISCUSSION

The relevance of adipose tissue *versus* skeletal muscle in mediating PPARγ function in glucose tolerance has been debated (10, 11, 34). PPARγ is a master regulator of adipogenesis (7, 35) whose induction, associated with the capability for fatty acid trapping, has been shown to represent an important contributor to the maintenance of systemic insulin sensitivity (12, 36). However, studies in mice with targeted loss of PPARγ in the skeletal muscle revealed development of severe insulin resistance in these animals (2). Despite development of fat and liver insulin resistance (2, 11), evidence was also obtained that, in these mice, PPARγ directly coordinates glucoregulatory responses in the skeletal muscle and this action is needed for the beneficial effects of PPARγ agonists in ameliorating insulin resistance conditions (10). Comprehensive and unbiased mRNA profiling studies in rats revealed that PPARγ activation has coordinate effects on gene expression in multiple insulin-sensitive tissues, with regulation of specific gene panels in each of these tissues (37).

However, in the skeletal muscle, the panel of the genes regulated by PPARγ is still incomplete, making the molecular details of PPARγ action on muscle glucoregulatory function unclear. In this study, we report that in mouse skeletal muscle tissue and

TABLE 1

Rosiglitazone effects on biochemical parameters of mice subjected to different dietary regimens

All data are presented as means ± S.E. Statistical differences were determined by one- or two-way analysis of variance as appropriate, and Bonferroni post hoc testing was performed when applicable. A p value of <0.05 was considered significant. ITT indicates insulin tolerance test; AUC indicates area under curve; CNV indicates copy number variation; CHOL indicates serum total cholesterol; TG indicates serum triglycerides. Data are means ± S.E. STD indicates standard diet mice; HFD indicates high fat diet mice; HFD+R indicates high fat diet mice after treatment with rosiglitazone 10 mg/kg/10 days, oral gavage.

	STD (n = 10)	HFD (n = 8)	HFD+R (n = 6)
Body weight	28.51 ± 0.99 g	39.11 ± 1.30 g[a]	39.84 ± 2.27 g
Food intake	3.16 ± 0.09 g/mouse/day	2.87 ± 0.2 g/mouse/day	2.40 ± 0.2 g/mouse/day
AUC ITT	9343.5 ± 424.5 mg/dl·120 min	21517.5 ± 1812.7 mg/dl·120 min[a]	14817 ± 1038.5 mg/dl·120 min[b]
PED/PEA-15	2.81 ± 2.1E-05 CNV	6.77 ± 1.23E-04 CNV[b]	5.25 ± 7.75E-05 CNV[c]
CHOL	102.5 ± 6.71 mg/dl	207.33 ± 17.48 mg/dl[b]	130.8 ± 15.73 mg/dl[c]
TG	95.4 ± 6.64 mg/dl	204.23 ± 26.74 mg/dl[b]	83.86 ± 9.97 mg/dl[b]
HDL	47.16 ± 6.70 mg/dl	68.87 ± 11.10 mg/dl	57.74 ± 5.33 mg/dl
LDL	6.25 ± 1.10 mg/dl	15.40 ± 2.30 mg/dl[d]	6.83 ± 0.68 mg/dl[c]
Glucose	107 ± 6.0 mg/dl	180 ± 11 mg/dl[a]	163 ± 6.0 mg/dl[c]
Insulin	0.36 ± 0.13 ng/ml	1.09 ± 0.2 ng/ml[a]	0.68 ± 0.32 ng/ml[c]

[a] Significant differences were between high fat diet mice *versus* standard diet mice and between high fat diet mice after treatment with rosiglitazone *versus* high fat diet mice. $p \leq 0.001$.
[b] $p \leq 0.01$.
[c] Data are indicated by t test.
[d] $p \leq 0.05$.

in L6 skeletal muscle cell line the PPARγ agonists Rtz and Ptz repress the expression of *ped/pea-15*, identifying this gene as a novel downstream target of PPARγ. Indeed, either preincubation with the PPARγ antagonist GW9662 or transfection with the dominant negative PPARγ mutant, $PPAR\gamma_{L468A/E471A}$ (24), completely blocked the Rtz effect.

Previous studies in mice and in humans demonstrated that PED/PEA-15 serves as a physiological regulator of glucose tolerance (13, 38). *PED/PEA-15* is transcriptionally up-regulated in type 2 diabetics as well as in their euglycemic offspring (17), determining insulin resistance in glucose disposal in the skeletal muscle mass (15). The mechanisms of *PED/PEA-15* transcriptional control have been only partially elucidated, but its repression by PPARγ agonists in skeletal muscle may contribute to the beneficial effects of these agents when administered to individuals with abnormalities in glucose tolerance. In support of these conclusions, we observed that, together with its action on *ped/pea-15* transcription, Rtz improved insulin-stimulated glucose uptake in the L6 cells, although both these effects were simultaneously impaired in cells expressing *ped/pea-15* under the control of an exogenous promoter. In addition, the *in vivo* studies reported in this work now show that high fat diet raised the expression of *ped/pea-15* in parallel with the development of insulin resistance, whereas Rtz simultaneously reversed both of these effects.

The finding that *ped/pea-15* is a target of PPARγ prompted us to further explore *in vitro* the details of PPARγ regulation of this gene. Previous studies in cells treated with TPA, a known activator of both AP-1 and NF-κB, revealed increased *ped/pea-15* expression (18), supporting the hypothesis that PPARγ brakes *ped/pea-15* transcription by transrepressing one or both of these transcription factors. Indeed, in the course of this study, we have functionally validated the presence of binding sequences for AP-1 and NF-κB at the promoter of *PED/PEA-15,* and the anti-inflammatory action of PPARγ is known to be mediated to a major extent via transrepression of these factors (39). Interestingly, supershift and ChIP experiments revealed that Rtz reduced *ped/pea-15* promoter occupancy by the c-jun moiety of the AP-1 transcriptional complex. In contrast, NF-κB presence at *ped/pea-15* promoter was unaffected in TZD-treated cells, indicating high specificity in the PPARγ-dependent transcriptional control of *ped/pea-15*. The observation that PPARγ inhibits Jun/AP-1 binding to DNA suggests a potential direct protein-protein interaction between PPARγ and c-Jun. A similar negative interference with AP-1 activity has been described for other nuclear receptors, such as the retinoic acid receptor (40) and the glucocorticoid receptor (41). In these reports, both the glucocorticoid receptor and retinoic acid receptor were shown to form a nonproductive complex with c-jun, leading to a decrease of AP-1 binding activity. Alternatively, PPARγ could block or destabilize an interaction between c-Jun and a cellular factor that facilitates DNA binding. Constructs bearing mutations at the CRE-like site of *PED/PEA-15* promoter, but not within the NF-κB-binding site, failed in affecting promoter activity when AP-1 and NF-κB were activated by TPA. Thus, AP-1 but not NF-κB is necessary for PPARγ control of the *PED/PEA-15* transcription. Furthermore, Rtz treatment in cells upon silencing of c-jun showed no effect on *ped/pea-15* expression, indicating that c-jun transrepression is sufficient for the PPARγ action. The mechanism responsible for the Rtz effect on *ped/pea-15* promoter occupancy by c-jun was not based on changes in the levels of c-jun itself. Alternatively, Rtz might impair ability of c-jun to bind to the *ped/pea-15* promoter, as forcing its occupancy by c-jun overexpression blocked the Rtz repression of *ped/pea-15*.

The chronic low grade inflammation induced by obesity is well recognized as a key trait of type 2 diabetes (42), as a number of inflammatory pathways are activated in classical insulin target tissues of these individuals (43, 44). These signaling cascades include the JNK/AP-1 network that is known to be down-regulated by PPARγ (39). However, genes that are ultimately involved in the impairment of glucose tolerance induced by inflammatory stimuli are still largely unknown. We now report that *ped/pea-15* expression is controlled by physiological levels of c-jun in the cells. Indeed, c-jun silencing with specific antisense impairs basal *ped/pea-15* expression. In addition, PPARγ activating anti-inflammatory agents regulate *ped/pea-15* by reducing c-jun occupancy at its promoter. These findings identify *ped/pea-15* as a gene whose transcription may change in response to common abnormalities typical of the low grade

unresolved inflammation associated with type 2 diabetes. Further studies assessing *ped/pea-15* function may offer previously unrecognized opportunities to identify these abnormalities.

Acknowledgments—We thank Dr. Mitchell Lazar (University of Pennsylvania, Philadelphia) for kindly providing the PPRE3-tk-luciferase construct. The dominant negative PPARγ expression vector was kindly provided by Dr. V. K. K. Chatterjee (University of Cambridge, Cambridge, UK). We also thank to Dr. Domenico Liguoro for helpful advice with cell culture technologies.

REFERENCES

1. Gurnell, M., and Chatterjee, V. K. (2004) Nuclear receptors in disease. Thyroid receptor β, peroxisome proliferator-activated receptor γ, and orphan receptors. *Essays Biochem.* **40,** 169–189
2. Kintscher, U., and Law, R. E. (2005) PPARγ-mediated insulin sensitization. The importance of fat *versus* muscle. *Am. J. Physiol. Endocrinol. Metab.* **288,** E287–E291
3. Rosen, E. D., and Spiegelman, B. M. (2001) PPARγ. A nuclear regulator of metabolism, differentiation, and cell growth. *J. Biol. Chem.* **276,** 37731–37734
4. Tontonoz, P., and Spiegelman, B. M. (2008) Fat and beyond: the diverse biology of PPARγ. *Annu. Rev. Biochem.* **77,** 289–312
5. Donath, M. Y., and Shoelson, S. E. (2011) Type 2 diabetes as an inflammatory disease. *Nat. Rev. Immunol.* **11,** 98–107
6. Frias, J. P., Yu, J. G., Kruszynska, Y. T., and Olefsky, J. M. (2000) Metabolic effects of troglitazone therapy in type 2 diabetic, obese, and lean normal subjects. *Diabetes Care* **23,** 64–69
7. Miyazaki, Y., Mahankali, A., Matsuda, M., Glass, L., Mahankali, S., Ferrannini, E., Cusi, K., Mandarino, L. J., and DeFronzo, R. A. (2001) Improved glycemic control and enhanced insulin sensitivity in type 2 diabetic subjects treated with pioglitazone. *Diabetes Care* **24,** 710–719
8. Nolan, J. J., Ludvik, B., Beerdsen, P., Joyce, M., and Olefsky, J. (1994) Improvement in glucose tolerance and insulin resistance in obese subjects treated with troglitazone. *N. Engl. J. Med.* **331,** 1188–1193
9. Raskin, P., Rappaport, E. B., Cole, S. T., Yan, Y., Patwardhan, R., and Freed, M. I. (2000) Rosiglitazone short-term monotherapy lowers fasting and post-prandial glucose in patients with type II diabetes. *Diabetologia* **43,** 278–284
10. Hevener, A. L., He, W., Barak, Y., Le, J., Bandyopadhyay, G., Olson, P., Wilkes, J., Evans, R. M., and Olefsky, J. (2003) Muscle-specific Pparγ deletion causes insulin resistance. *Nat. Med.* **9,** 1491–1497
11. Norris, A. W., Chen, L., Fisher, S. J., Szanto, I., Ristow, M., Jozsi, A. C., Hirshman, M. F., Rosen, E. D., Goodyear, L. J., Gonzalez, F. J., Spiegelman, B. M., and Kahn, C. R. (2003) Muscle-specific PPARγ-deficient mice develop increased adiposity and insulin resistance but respond to thiazolidinediones. *J. Clin. Invest.* **112,** 608–618
12. Shulman, G. I. (2000) Cellular mechanisms of insulin resistance. *J. Clin. Invest.* **106,** 171–176
13. Condorelli, G., Vigliotta, G., Iavarone, C., Caruso, M., Tocchetti, C. G., Andreozzi, F., Cafieri, A., Tecce, M. F., Formisano, P., Beguinot, L., and Beguinot, F. (1998) PED/PEA-15 gene controls glucose transport and is overexpressed in type 2 diabetes mellitus. *EMBO J.* **17,** 3858–3866
14. Fiory, F., Formisano, P., Perruolo, G., and Beguinot, F. (2009) Frontiers. PED/PEA-15, a multifunctional protein controlling cell survival and glucose metabolism. *Am. J. Physiol. Endocrinol. Metab.* **297,** E592–E601
15. Condorelli, G., Vigliotta, G., Trencia, A., Maitan, M. A., Caruso, M., Miele, C., Oriente, F., Santopietro, S., Formisano, P., and Beguinot, F. (2001) Protein kinase C (PKC)-α activation inhibits PKC-ζ and mediates the action of PED/PEA-15 on glucose transport in the L6 skeletal muscle cells. *Diabetes* **50,** 1244–1252
16. Viparelli, F., Cassese, A., Doti, N., Paturzo, F., Marasco, D., Dathan, N. A., Monti, S. M., Basile, G., Ungaro, P., Sabatella, M., Miele, C., Teperino, R., Consiglio, E., Pedone, C., Beguinot, F., Formisano, P., and Ruvo, M. (2008) Targeting of PED/PEA-15 molecular interaction with phospholipase D1 enhances insulin sensitivity in skeletal muscle cells. *J. Biol. Chem.* **283,** 21769–21778
17. Valentino, R., Lupoli, G. A., Raciti, G. A., Oriente, F., Farinaro, E., Della Valle, E., Salomone, M., Riccardi, G., Vaccaro, O., Donnarumma, G., Sesti, G., Hribal, M. L., Cardellini, M., Miele, C., Formisano, P., and Beguinot, F. (2006) The PEA15 gene is overexpressed and related to insulin resistance in healthy first-degree relatives of patients with type 2 diabetes. *Diabetologia* **49,** 3058–3066
18. Perfetti, A., Oriente, F., Iovino, S., Alberobello, A. T., Barbagallo, A. P., Esposito, I., Fiory, F., Teperino, R., Ungaro, P., Miele, C., Formisano, P., and Beguinot, F. (2007) Phorbol esters induce intracellular accumulation of the anti-apoptotic protein PED/PEA-15 by preventing ubiquitinylation and proteasomal degradation. *J. Biol. Chem.* **282,** 8648–8657
19. Ungaro, P., Teperino, R., Mirra, P., Longo, M., Ciccarelli, M., Raciti, G. A., Nigro, C., Miele, C., Formisano, P., and Beguinot, F. (2010) Hepatocyte nuclear factor (HNF)-4α-driven epigenetic silencing of the human PED gene. *Diabetologia* **53,** 1482–1492
20. Schlingensiepen, K. H., Schlingensiepen, R., Kunst, M., Klinger, I., Gerdes, W., Seifert, W., and Brysch, W. (1993) Opposite functions of jun-B and c-jun in growth regulation and neuronal differentiation. *Dev. Genet.* **14,** 305–312
21. Ungaro, P., Teperino, R., Mirra, P., Cassese, A., Fiory, F., Perruolo, G., Miele, C., Laakso, M., Formisano, P., and Beguinot, F. (2008) Molecular cloning and characterization of the human PED/PEA-15 gene promoter reveal antagonistic regulation by hepatocyte nuclear factor 4α and chicken ovalbumin upstream promoter transcription factor II. *J. Biol. Chem.* **283,** 30970–30979
22. Condorelli, G., Trencia, A., Vigliotta, G., Perfetti, A., Goglia, U., Cassese, A., Musti, A. M., Miele, C., Santopietro, S., Formisano, P., and Beguinot, F. (2002) Multiple members of the mitogen-activated protein kinase family are necessary for PED/PEA-15 anti-apoptotic function. *J. Biol. Chem.* **277,** 11013–11018
23. DuBois, R. N., Gupta, R., Brockman, J., Reddy, B. S., Krakow, S. L., and Lazar, M. A. (1998) The nuclear eicosanoid receptor, PPARγ, is aberrantly expressed in colonic cancers. *Carcinogenesis* **19,** 49–53
24. Gurnell, M., Wentworth, J. M., Agostini, M., Adams, M., Collingwood, T. N., Provenzano, C., Browne, P. O., Rajanayagam, O., Burris, T. P., Schwabe, J. W., Lazar, M. A., and Chatterjee, V. K. (2000) A dominant-negative peroxisome proliferator-activated receptor γ (PPARγ) mutant is a constitutive repressor and inhibits PPARγ-mediated adipogenesis. *J. Biol. Chem.* **275,** 5754–5759
25. Tremblay, F., and Marette, A. (2001) Amino acid and insulin signaling via the mTOR/p70 S6 kinase pathway. A negative feedback mechanism leading to insulin resistance in skeletal muscle cells. *J. Biol. Chem.* **276,** 38052–38060
26. Wheatley, K. E., Nogueira, L. M., Perkins, S. N., and Hursting, S. D. (2011) Differential effects of calorie restriction and exercise on the adipose transcriptome in diet-induced obese mice. *J. Obes.* **2011,** 265417
27. Miele, C., Raciti, G. A., Cassese, A., Romano, C., Giacco, F., Oriente, F., Paturzo, F., Andreozzi, F., Zabatta, A., Troncone, G., Bosch, F., Pujol, A., Chneiweiss, H., Formisano, P., and Beguinot, F. (2007) PED/PEA-15 regulates glucose-induced insulin secretion by restraining potassium channel expression in pancreatic beta-cells. *Diabetes* **56,** 622–633
28. Bradford, M. M. (1976) A rapid and sensitive method for the quantitation of microgram quantities of protein utilizing the principle of protein-dye binding. *Anal. Biochem.* **72,** 248–254
29. Livak, K. J., and Schmittgen, T. D. (2001) Analysis of relative gene expression data using real time quantitative PCR and the $2(-\Delta\Delta C(T))$ Method. *Methods* **25,** 402–408
30. Whelan, J. A., Russell, N. B., and Whelan, M. A. (2003) A method for the absolute quantification of cDNA using real time PCR. *J. Immunol. Methods* **278,** 261–269
31. Dignam, J. D., Lebovitz, R. M., and Roeder, R. G. (1983) Accurate transcription initiation by RNA polymerase II in a soluble extract from isolated mammalian nuclei. *Nucleic Acids Res.* **11,** 1475–1489
32. Ricote, M., and Glass, C. (2007) PPARs and molecular mechanism of transrepression. *Biochim. Biophys. Acta* **1771,** 926–935
33. Medcalf, R. L., Rüegg, M., and Schleuning, W. D. (1990) A DNA motif

related to the cAMP-responsive element and an exon-located activator protein-2-binding site in the human tissue-type plasminogen activator gene promoter cooperate in basal expression and convey activation by phorbol ester and cAMP. *J. Biol. Chem.* **265,** 14618–14626
34. Zierath, J. R., Ryder, J. W., Doebber, T., Woods, J., Wu, M., Ventre, J., Li, Z., McCrary, C., Berger, J., Zhang, B., and Moller, D. E. (1998) Role of skeletal muscle in thiazolidinedione insulin sensitizer (PPARγ agonist) action. *Endocrinology* **139,** 5034–5041
35. Kubota, N., Terauchi, Y., Miki, H., Tamemoto, H., Yamauchi, T., Komeda, K., Satoh, S., Nakano, R., Ishii, C., Sugiyama, T., Eto, K., Tsubamoto, Y., Okuno, A., Murakami, K., Sekihara, H., Hasegawa, G., Naito, M., Toyoshima, Y., Tanaka, S., Shiota, K., Kitamura, T., Fujita, T., Ezaki, O., Aizawa, S., Kadowaki, T., *et al.* (1999) PPARγ mediates high fat diet-induced adipocyte hypertrophy and insulin resistance. *Mol. Cell* **4,** 597–609
36. Samuel, V. T., and Shulman, G. I. (2012) Mechanisms for insulin resistance: common threads and missing links. *Cell* **148,** 852–871
37. Way, J. M., Harrington, W. W., Brown, K. K., Gottschalk, W. K., Sundseth, S. S., Mansfield, T. A., Ramachandran, R. K., Willson, T. M., and Kliewer, S. A. (2001) Comprehensive messenger ribonucleic acid profiling reveals that peroxisome proliferator-activated receptor γ activation has coordinate effects on gene expression in multiple insulin-sensitive tissues. *Endocrinology* **142,** 1269–1277
38. Vigliotta, G., Miele, C., Santopietro, S., Portella, G., Perfetti, A., Maitan, M. A., Cassese, A., Oriente, F., Trencia, A., Fiory, F., Romano, C., Tiveron, C., Tatangelo, L., Troncone, G., Formisano, P., and Beguinot, F. (2004) Overexpression of the *ped/pea-15* gene causes diabetes by impairing glucose-stimulated insulin secretion in addition to insulin action. *Mol. Cell. Biol.* **24,** 5005–5015
39. Blanquart, C., Barbier, O., Fruchart, J. C., Staels, B., and Glineur, C. (2003) Peroxisome proliferator-activated receptors. Regulation of transcriptional activities and roles in inflammation. *J. Steroid Biochem. Mol. Biol.* **85,** 267–273
40. Schüle, R., Rangarajan, P., Yang, N., Kliewer, S., Ransone, L. J., Bolado, J., Verma, I. M., and Evans, R. M. (1991) Retinoic acid is a negative regulator of AP-1 responsive genes. *Proc. Natl. Acad. Sci. U.S.A.* **88,** 6092–6096
41. Jonat, C., Rahmsdorf, H. J., Park, K. K., Cato, A. C., Gebel, S., Ponta, H., and Herrlich, P. (1990) Antitumor promotion and anti-inflammation. Down-modulation of AP-1 (Fos/jun) activity by glucocorticoid hormone. *Cell* **62,** 1189–1204
42. Osborn, O., and Olefsky, J. M. (2012) The cellular and signaling networks linking the immune system and metabolism in disease. *Nat. Med.* **18,** 363–374
43. Itani, S. I., Ruderman, N. B., Schmieder, F., and Boden, G. (2002) Lipid-induced insulin resistance in human muscle is associated with changes in diacylglycerol, protein kinase C, and IκB-α. *Diabetes* **51,** 2005–2011
44. Bandyopadhyay, G. K., Yu, J. G., Ofrecio, J., and Olefsky, J. M. (2005) Increased p85/55/50 expression and decreased phosphatidylinositol 3-kinase activity in insulin-resistant human skeletal muscle. *Diabetes* **54,** 2351–2359